Probability of Liquefaction for H-Area Savannah River Site

By

R.C. Lee, M.D. McHood, and M.R. Lewis

Approved by: Lawrence A Salomone

Lawrence A. Salomone
SRS Chief Geotechnical Engineer

Westinghouse Savannah River, Inc.
Savannah River Site
Aiken, SC 29808

Site Geotechnical Services
Geotechnical Engineering Group

This document was prepared in conjunction with work accomplished under Contract No. DE-AC09-96SR18500 with the U.S. Department of Energy.

DISCLAIMER

LIST OF ACRONYMS

ASHLE	Advanced Seismic Hazard Liquefaction Evaluation
CPT	cone penetrometer testing
CPTU	piezocone penetrometer test soundings
CSR	cyclic stress ratio (τ_{ave} / σ'_v)
CSRN	cyclic stress ratio normalized to magnitude 7.5
CRR	cyclic resistance ratio
DOE	United States Department of Energy
EPRI	Electric Power Research Institute
τ_{ave}	effective shear stress
σ'_v	effective overburden pressure
GSA	General Separations Area
HTF	H-Tank Farm
ITP	In-Tank Precipitation Facility
LLNL	Lawrence Livermore National Laboratory
M-bar	average earthquake magnitude
MH	high magnitude
ML	low magnitude
MM	median magnitude
N_{60}	standard penetration blowcount normalized to 60% energy
$(N_1)_{60}$	standard penetration blowcount normalized for overburden pressure and 60% energy
NRC	United States Nuclear Regulatory Commission
OCR	overconsolidation ratio
PC-3	performance category 3
PC-4	performance category 4
PGA	peak ground acceleration
POL	probability of liquefaction
POO	probability of occurrence
PSHA	probabilistic seismic hazard assessment
RTF	Replacement Tritium Facility
SAF	soil amplification factor/function
SGS	Site Geotechnical Services
SPT	standard penetration test
SRS	Savannah River Site
USGS	United States Geological Survey
WSRC	Westinghouse Savannah River Company

1.0 INTRODUCTION

In 1995 WSRC completed the geotechnical assessment for the In-Tank Precipitation Facility (ITP) and the H-Tank Farm at the Savannah River Site (SRS). As part of that assessment, a probabilistic liquefaction evaluation for the Tobacco Road soils was completed. The ITP evaluation of capacity was based on site-specific soil properties as determined from normalized standard penetration test (SPT) blowcount ($(N_1)_{60}$), and cone penetrometer testing (CPT). A SRS bedrock probabilistic seismic hazard assessment (PSHA) developed by the Electric Power Research Institute (EPRI) was used together with a site-specific convolution analysis to develop seismic demand. At the time of the original ITP evaluation this was the only hazard study available with deaggregated results. The DOE and WSRC jointly agreed to proceed using this single hazard study. The results showed that the annual liquefaction hazard was less than 10^{-5}, which met the performance goal for ITP and performance category 4 (PC-4). Since that evaluation a significant amount of work has been done at the SRS related to site-wide soil properties and site-wide ground motion. In addition, the Lawrence Livermore National Laboratory (LLNL) SRS bedrock PSHA (Bernreuter, 1997) was revised in 1996, new SRS soil amplification functions (SAFs) were developed in 1997 (WSRC, 1997), and the United States Geological Survey (USGS) developed a SRS hard-rock site PSHA (Frankel, 1999) consistent with the National Map. With the possibility of new missions being sited at SRS and the need to understand the new information regarding the USGS hazard, it was concluded that the probability of liquefaction needed re-evaluation. This assessment re-evaluates the probability of liquefaction building upon work performed to date including:

- In Tank Precipitation Facility (ITP) and H-Tank Farm (HTF) Geotechnical Report (WSRC, 1995),
- Savannah River Site Replacement Tritium Facility (233H) Geotechnical Investigation (WSRC, 1993),
- SRS Seismic Response Analysis and Design Basis Guidelines (WSRC, 1997),
- Soil Surface Seismic Hazard and Design Basis Guidelines for Performance Category 1 & 2 SRS Facilities (WSRC, 1998),
- EPRI Seismic Siting Decision Process (NEI, 1994),
- LLNL Fission Energy and Systems Safety Program (Bernreuter, 1997), and
- Results of USGS calculation of SRS PSHA (Frankel, 1999).

2.0 SCOPE

The specific scope of the work included the following:

1. Implement probability of liquefaction methodology and check the computation against the results from the 1995 ITP evaluation, and
2. Utilizing the results of the existing cone penetration test soundings in H-Area, compute the annual probability of liquefaction.

The original scope for this task was to evaluate the liquefaction potential for both H- and F-Areas. However, it was concluded that, since the subsurface conditions in H-Area are less favorable than F-Area (in terms of depth to the water table and shear wave velocity), the results from H-Area would be a bounding (lower bound or highest probability) case. Consequently, this study focuses on the annual probability of liquefaction for H-Area. The study was not performed for any particular project nor will the result be used in any other facility-specific analysis. If a facility requires the annual liquefaction hazard to be determined, this study will serve as the basis for that effort.

3.0 METHODOLOGY

3.1 Evaluation of Probability of Liquefaction

The basic methodology used for this assessment was derived from the previously completed ITP geotechnical evaluation (WSRC, 1995). In the ITP geotechnical evaluation, a methodology was developed to evaluate the probability of liquefaction (POL) of a subsurface soil layer or formation. That methodology uses a PSHA evaluated for bedrock outcrop, a determination of seismically induced cyclic stress ratios (CSR) for the soil profile using a suite of convolution analyses from bedrock, an evaluation of the distribution of normalized SPT blowcount (i.e., $(N_1)_{60}$) for the soil section, and the POL given seismically induced CSR and normalized blowcount available in the literature.

In this study and the 1995 ITP evaluation, the probability of liquefaction is obtained by evaluating the probability of occurrence of specific earthquakes and the probability of liquefaction given the occurrence of a specific earthquake. Given those evaluations, the probability of liquefaction for a specific earthquake is:

$$P_E(L) = P[L \mid E]\, P[E]$$

Where $P_E(L)$ is the probability of liquefaction as a result of an earthquake; $P[L \mid E]$ is the conditional probability of liquefaction given that the earthquake occurs; and P[E] is the probability that the earthquake occurs. The total overall probability of liquefaction is obtained by summing over all possible earthquakes, as follows:

$$P[L] = \sum_{E} P[L \mid E]\, P[E]$$

The methodology presented herein uses the model for conditional probability of liquefaction developed by Liao, et al, (1988). The model was developed based on statistical analyses of a data catalog consisting of 278 observed cases of liquefaction/no liquefaction in Holocene deposits, for 40 earthquakes. The Liao et al. models for clean and silty sand are shown in Figures 1a and 1b.

From the Liao et al. model, the probability of liquefaction can be obtained once the normalized standard penetration test blowcount $(N_1)_{60}$ and the normalized cyclic stress ratio (CSRN) are known. For this assessment the $(N_1)_{60}$ is determined from site-specific correlations with the tip resistance (q_t), sleeve friction (f_s) and pore pressure (u) results from piezocone penetrometer test soundings (CPTU) (see Section 3.5). The seismically induced CSRs were determined from convolution analysis using SRS soil profiles from WSRC (1997) (see Section 3.6).

The probabilities discussed above combine to form the following liquefaction hazard formulation (WSRC, 1995):

$$P[L] = \sum_i \sum_j \sum_k \sum_l P[L \mid CSRN_k(\bar{v}_i, m_j), ((N_1)_{60})_l] * P[v = \bar{v}_i, m_j] * [W_{CSRN}]_k * [W_{N160}]_l \qquad \text{(Eq. 1)}$$

(1) (2) (3) (4)

Term (1) is computed directly from the results of Liao et al., (1988). Term (2) is derived from the hard-rock PSHA by computing differences of the PSHA disaggregation matrices at each level of motion v_i corresponding to magnitude m_j. Terms (3) and (4) are weights dependent on the distributions of cyclic stress ratio and $(N_1)_{60}$.

3.2 SRS Hard-Rock PSHAs for Liquefaction Analysis

Three hard-rock PSHAs were used to evaluate the probability of liquefaction in this study. The EPRI PSHA (NEI, 1994), used in the ITP evaluation (WSRC, 1995), is used for a direct comparison to prior probabilistic assessments. The other hard-rock PSHAs completed for the SRS by LLNL (Bernreuter, 1997) and the USGS (Frankel, 1999) were also used in the liquefaction assessments. Note that although the LLNL PSHA was available in 1995, the PSHA disaggregation was not available and consequently, the LLNL probability of liquefaction was not evaluated in 1995. The USGS PSHA was also not available in 1995. Site-wide SRS surface design basis spectra have been developed using evaluations of the hard-rock EPRI and LLNL PSHAs (WSRC, 1997; WSRC, 1998). The PSHA oscillator frequency used was 2.5 Hz, the same frequency used for the ITP evaluation.

3.3 H-Area Geology

Existing cone penetrometer soundings and borings were used to examine the lithology and geology and to layer the subsurface for the entire H-Area. Examining small subsets within H-Area (e.g. ITP or RTF) allows identification of laterally continuous layers having similar engineering properties. In contrast, across the entire H-Area, laterally continuous layers having the same engineering properties are difficult to identify. This leads to the conclusion that a single laterally continuous weak layer may not be present across H-Area. However, common markers such as the Tan Clay Unit can be identified at many of the CPT and boring locations, and it was possible to layer H-Area by geologic formation. For this effort, the Upland, Tobacco Road, Dry Branch, and the top of the Santee Formations were identified (WSRC, 2000a).

3.4 Determination of Critical Layer for Liquefaction

The relationship between $(N_1)_{60}$, fines, and cyclic resistance ratio (CRR) developed by Seed et al. (1984) was used to determine layers most susceptible to liquefaction (see Figure 2). The "τ_{ave} / σ'_o" shown in Figure 2, termed CRR, should not be confused with seismically induced cyclic stress ratio (i.e., CSR). The CRR represents the soil capacity while the CSR represents seismic demand. The ratio of CRR to CSR would be the factor of safety against liquefaction. Since the Seed et al. relationship does not account for age or magnitude, the CRR is only a relative measure of resistance to liquefaction, and therefore was only used to help identify critical layers.

The $(N_1)_{60}$ and corresponding fines content are necessary to use the Seed et al. relationship. Similar to the evaluation performed for the ITP project, CPTU results were used to estimate $(N_1)_{60}$. The $(N_1)_{60}$ was estimated using relationships developed specifically for SRS soils, as opposed to the methodology developed specifically for ITP. N_{60} was computed using Equations 2 and 3. These equations were developed by correlating SPT results with nearby CPTU results (WSRC, 2000b).

$$N_{60} = \frac{q_c}{8.85 - 1.85 I_c} \qquad \text{(Eq. 2)}$$

$$I_c = \sqrt{\left(3.25 - \log[Q_t(1 - B_q)]\right)^2 + \left(1.5(1 + \log Fr)\right)^{2.25}} \qquad \text{(Eq. 3)}$$

Where: Q_t is normalized tip resistance $Q_t = (q_t - \sigma_v)/\sigma'_v$
B_q is pore pressure ratio $B_q = (u - u_o) / (q_t - \sigma_v)$
Fr is stress normalized friction ratio $Fr = [(f_s/q_t - \sigma_v) \times 100]$
q_c is uncorrected CPTU tip stress
q_t is CPTU tip stress corrected for unequal area effects
f_s is CPTU sleeve friction

The N_{60} values were normalized to $(N_1)_{60}$ values using Equation 4 (Liao and Whitman, 1986).

$$(N_1)_{60} = N_{60} \times [1 / (\sigma_v')]^{0.5} \qquad \text{(Eq. 4)}$$

In order to account for the increase in liquefaction resistance due to increase in fines content, as proposed in the Seed et al. relationship, it is also necessary to determine fines content corresponding to the $(N_1)_{60}$ values. Fines content was also estimated using CPTU data as follows:

$$\text{Fines} = 0.3(I_{fc}^{3.5}) + 2 \qquad \text{(Eq. 5)}$$

$$I_{fc} = 1.1 + [(1.5 - \log Q_t)^2 + (\log Fr + 1.7)^2]^{0.5} \qquad \text{(Eq. 6)}$$

Where Q_t and Fr are the same as those provided for Equation 3. Equations 5 and 6 were developed by correlating laboratory determined fines content from borings with nearby CPTU results.

The estimated $(N_1)_{60}$ and fines content were used to determine CRR using the Seed et al. relationship. Three dimensional images of CRR were developed without regard to geologic or engineering layer to identify layers most susceptible to liquefaction. Data collected at greater depths (i.e., within the Santee Unit or deeper) and above the water table were not considered. As with the attempt to identify laterally continuous layers having similar engineering properties across H-Area (Section 3.3), the CRR results showed no discernible layers that were laterally continuous across H-Area. Within the H-Area geologic units, the CRR varies both vertically and laterally. However, as a whole, the Tobacco Road Formation appears to have more "zones" of lower CRR than the Dry Branch. Thus, the critical layer selected to represent H-Area was the saturated portion of the Tobacco Road. In instances where the top of the Tobacco Road was above the water table, the water table was taken as the top of the critical layer. On average, the H-Area critical layer was about 25 feet thick having an average elevation of between approximately 255 ft msl and 230 ft msl (see Figure 3). This corresponds roughly to the layer analyzed at ITP having an average elevation of between approximately 247 ft msl and 224 ft msl.

3.5 Determination of Soil Capacity $(N_1)_{60}$

In order to utilize published probabilistic liquefaction curves (Liao et al., 1988) the CPTU results were converted to equivalent $(N_1)_{60}$ values using equations 2, 3 and 4 in Section 3.4. The $(N_1)_{60}$ mean and standard deviation were determined for the critical layer (WSRC, 2000c) along with histograms of the data and log transformed data (Figures 4 and 5).

The conditional probability of liquefaction model developed by Liao et al. was based on data entirely from the Holocene (recent) period. The soils in question at the SRS are of the Miocene period and as such, have significantly higher cyclic strength than Holocene soils. Thus, modifications to the Liao model were required. Specifically, corrections are required to account for aging, overconsolidation and sample disturbance. Each is discussed below.

3.5.1 Aging

Aging has been addressed at the SRS through extensive laboratory testing of recovered samples from the Tobacco Road, Dry Branch and Santee Formations. The results show that the soils at the SRS have significantly higher cyclic shear strengths than similar soils of the Holocene period. The results have been used to develop SRS site-specific curves accounting for aging of the soils at the SRS. The resulting average increase in strength for the SRS soils over the Holocene soils is 1.35 (WSRC, 1995).

3.5.2 Overconsolidation

The site-specific cyclic shear strength curves are based on a conservative overconsolidation ratio (OCR) estimate of 2. A best estimate of the OCR for the Tobacco Road Formation in H-Area is 3. Thus, the actual strength of the material is greater. For a "best estimate" of cyclic shear strength, the strength increase would be 1.09 times greater (WSRC, 1995).

3.5.3 Sample Disturbance

The SRS curves do not account for potential loss of strength due to sampling disturbance. It is well known that even the most carefully planned and implemented sampling and testing program will result in disturbance to the recovered samples. It is also well known that sample disturbance reduces the laboratory-derived strength determinations. For site-specific deterministic liquefaction potential determinations, these effects are conservatively ignored. For this study however, the affects are considered in an effort to obtain a "best estimate" result.

Strength losses of up to 30% can be realized due to sample disturbance (Singh, et al., 1979). Thus, to account for these potential losses, a correction factor of 1.3 is recommended (WSRC, 1995).

Combining the factors from aging, overconsolidation and sample disturbance results in an overall factor of 1.9. This factor was applied to the Liao model for the probabilistic assessment.

3.6 Seismic Demand (CSRN)

Earthquake demand or Cyclic Stress Ratio (CSR) is defined as effective shear stress (τ_{ave}) divided by effective overburden pressure (σ'_v). A soil unit weight of 120 pcf was used to compute σ'_v with a water table depth of 25 feet. This is a conservative assumption as the water table is generally 25 feet or deeper in H-Area. A shallow water table results in lower σ'_v.

The CSRs were computed using previously developed bedrock motions and soil models representative of the General Separations Area (GSA) at SRS (WSRC, 1997). The bedrock control motions cover a range of magnitudes, distances and peak ground accelerations. The control motions are convolved through the soil to compute the average distribution of CSR for each layer in the soil model. As the critical layer is thicker (about 25 ft thick) than the convolution model layers (each about 10 ft thick), the CSR for the critical layer is determined by averaging the appropriate CSRs over the critical layer depth range. The control motion spectra are computed for a large range of hypothetical earthquakes so tables of CSR distributions can be interpolated. Thus, by differencing the PSHA disaggregation, the probability of occurrence of a specific level of bedrock motion is obtained corresponding to a range of earthquake magnitude and distance. The corresponding CSR distribution is then determined from the interpolated tables.

Convolution analysis used to compute CSRs is consistent with the 1997 SRS seismic design spectra (WSRC, 1997). Bedrock spectra and CSRs were computed for three magnitude levels (ML, MM, MH) and eight levels of peak ground acceleration (PGA) covering the range 0.05-0.75g. Because the site-specific CSRs cover a limited range of bedrock motions, the CSR distributions were extrapolated to lower and higher control motions. The lower control motion extrapolations (for PGA < 0.05) are not critical to the final result. The higher control motion extrapolations (for PGA > 0.75g) could impact the final results by underestimating or overestimating the CSR demand. For the EPRI, LLNL, and USGS PSHAs, less than about 10% of the POL contributions are made from control motion ranges that use extrapolated ranges of CSR. We recommend that if facility-specific POL is to be estimated that the site-specific database be expanded to larger ranges of control motions to eliminate or reduce the CSR extrapolation.

Before the CSR distributions can be used in conjunction with the Liao model they must be normalized for earthquake magnitude. Table 1 presents the Arango (1994; 1996) magnitude scaling factors (MSFs) used to normalize the CSRs to CSRNs. Figure 6 presents several MSFs that have been proposed by various investigators (NCEER, 1997). Also presented in Figure 6 is the range of MSFs recommended from the NCEER workshop. The Arango MSFs used for this assessment (denoted in Figure 6 by an open diamond) fall in the middle of the recommended range for most of the magnitudes and overall the Arango MSFs approximate a mean or "best estimate".

4.0 RESULTS

4.1 Validation of Liquefaction Hazard Implementation

Computer code LIQHAZ was developed specifically for the methodology used in this study. Advanced Seismic Hazard Liquefaction Evaluation (ASHLE) was the computer code used to compute probability of liquefaction for ITP evaluation (WSRC, 1995). There are computational differences in application of the probability of liquefaction methodology between LIQHAZ and ASHLE. LIQHAZ uses the full magnitude and distance disaggregation to evaluate the POL whereas ASHLE uses M-bar and D-bar, the mean earthquake magnitudes and distances controlling the hazard for a given level of ground motion. In addition, LIQHAZ uses an interpolation scheme to compute smoother values of the probability of occurrence disaggregation matrix.

In order to validate the liquefaction hazard implementation, the probability of liquefaction for the ITP site was calculated using LIQHAZ for comparison to values obtained in WSRC (1995). Seismic demand and capacity input for LIQHAZ, was similar to the data used by WSRC (1995). The EPRI PSHA for 2.5 Hz spectral acceleration was used to define motions at bedrock. Statistical distributions on CSRs were taken from WSRC (1995) where convolution analyses were used to compute suites of distributions of CSRs for the ITP Tobacco Road formation. Thus, for each level of bedrock motion, there were corresponding CSR distributions. The soil strength factor was taken as 1.9 (product of age x OCR x disturbance factors) WSRC (1995).

The Arango (1994; 1996) earthquake magnitude scaling factors were used (Table 1). The Tobacco Road soil capacity was taken as the combined simulated and measured $(N_1)_{60}$ distributions. The Liao et al. (1988) probability of liquefaction model for silty sand was used. Input for the validation (i.e., case 1) is summarized in Table 2.

The table below compares the probability of liquefaction results using LIQHAZ, in conjunction with the input data described above, to the ITP evaluation (WSRC, 1995).

PSHA	Soil Strength Factor	Geologic Formation	Magnitude Scaling Factor	Liao P[L] Model	POL LIQHAZ '95 ITP data	POL ASHLE '95 ITP data
EPRI	1.9	Tobacco Rd.	Arango	Silty Sand	4.90e-6	2.25e-6
LLNL	1.9	Tobacco Rd.	Arango	Silty Sand	3.57e-5	-

The EPRI POL results using LIQHAZ are approximately double the results using ASHLE. In light of the differences in program approach, these results are considered to be in general agreement. The results suggest that not accounting for the complete hazard disaggregation can result in an underestimate of the probability of liquefaction. The LLNL result was unavailable in the 1995 ASHLE evaluation. The LIQHAZ POL result using the LLNL PSHA (3.57e-5) is nearly an order of magnitude higher than the EPRI POL (4.90e-6).

4.2 Evaluation of ITP Probability of Liquefaction Using Site-Wide CSRs

Using the ITP subset of the H-Area CPTU data, the POL for ITP was also evaluated using soil capacity (i.e., $(N_1)_{60}$) and seismic demand (i.e., CSRN) developed for this study. In this instance, the seismic demand is consistent with the site-wide spectra development (WSRC, 1997).

For the ITP evaluation using site-wide seismic demand, the input was as follows: (1) the EPRI 2.5 Hz PSHA was used to define motions at bedrock; (2) the suite of CSR distributions were computed for Tobacco Road formation using a depth to water table of 25 ft; (3) soil strength factor was taken as 1.9; (4) the earthquake magnitude scaling factor used was Arango (1994; 1996); 5) Tobacco Road soil capacity was the CPT estimated $(N_1)_{60}$ distribution; and (6) the Liao et al. (1988) probability of liquefaction model for a silty sand. Table 2 summarizes the changes between this run (case 3) and the validation runs (case 1) discussed in Section 4.1.

The table below compares the probability of liquefaction results using LIQHAZ, in conjunction with the input data described above, to the ITP LIQHAZ evaluation using 1995 input discussed in Section 4.1.

PSHA	Soil Strength Factor	Geologic Formation	Magnitude Scaling Factor	Liao P[L] Model	POL LIQHAZ Current ITP data	POL LIQHAZ '95 ITP data
EPRI	1.9	Tobacco Rd.	Arango	Silty Sand	4.98e-6	4.90e-6

The EPRI POL for the ITP using seismic demand and soil capacity developed for this study is only slightly higher than the evaluation using the 1995 input. An evaluation of the input shows that both the seismic demand and the soil capacity have increased somewhat. These differences compensate and produce a result similar to the result using the ITP '95 demand and capacity. The seismic demand has increased due to three primary differences: (1) dynamic properties (i.e., strain dependent shear modulus and damping), (2) bedrock shear wave velocity, and (3) depth to water table. GEI, Inc. dynamic properties were used in the WSRC (1995) convolution analyses, and dynamic properties derived by the University of Texas (WSRC, 1996) were used in the SRS site-wide convolution analyses used herein. The GEI, Inc. dynamic properties have higher damping at low strain levels and consequently result in a lower predicted CSR than those developed using the University of Texas derived dynamic properties (see Figure 7). The WSRC (1995) convolution analyses used a bedrock shear-wave velocity of 8,000 ft/sec, significantly lower than the median value of 11,500 ft/sec used for this study. This bias would tend to reduce spectral amplification and also reduce CSR. The depth to water table used in the WSRC (1995) analysis was greater than that used herein, creating an additional bias that would tend to reduce the CSR.

In examining the differences between the ITP seismic demand (WSRC, 1995) and the WSRC (1997) seismic demand, convolution analyses were re-calculated for one of the twenty 1995 ITP soil models. The ITP soil model used was C18CFE. Calculations were rerun using: bedrock shear-wave velocity of 11,500 ft/sec, and the University of Texas derived (WSRC, 1996) dynamic soil properties (i.e., strain dependent shear modulus and damping). Figure 8 shows how increasing the bedrock shear wave velocity to 11,500 ft/sec in the ITP convolution analyses generally increases the CSR. Figure 9 shows how using the WSRC (1996) dynamic shear modulus and damping generally increases the CSR. Figure 10 presents the combined effect of both increasing the bedrock shear wave velocity and using the WSRC (1996) dynamic properties. Figure 11 shows how depth to water table affects the CSR. The two CSR (i.e., τ_{ave} / σ'_v) results shown in Figure 11 were calculated using the same shear stress (τ_{ave}) in the numerator, but calculating the effective overburden pressure using a water table depth of 25 and 50 feet. The shallow water table has the higher CSR.

Figure 12 shows the 1995 ITP soil capacity (i.e., measured and simulated $(N_1)_{60}$ values). Figure 13 shows the ITP soil capacity based on the current methodology, which uses data from 20 ITP CPTU in conjunction with Equations 2 through 4. Comparing Figures 12 and 13 shows an increase in $(N_1)_{60}$. This increase is likely due to the change in methodology for determining $(N_1)_{60}$ as well as differences in the top and bottom of the layer analyzed and an increase in the size of the data set, (7114 $(N_1)_{60}$ values with the current methodology as opposed to 71 $(N_1)_{60}$ values used in 1995). The new increased earthquake demand and new increased soil capacity are compensating differences that produce a result (POL of 4.98e-6) similar to that obtained when using the 1995 earthquake demand and soil capacity (POL of 4.90e-6).

4.3 Evaluation of H-Area Probability of Liquefaction Using LIQHAZ

For the H-Area POL assessment, the seismic demand, soil capacity, and correction factors were the same as those used in the ITP analysis described in Section 4.2. The only differences were: (1) additional hard-rock PSHAs conducted by LLNL and USGS were used; (2) the larger H-Area wide set of Tobacco Road soil capacity data were used; and (3) additional Liao et al. (1988) probability models representing clean and undifferentiated sands were used. Table 2 summarizes the changes between these runs and the other runs discussed previously in Sections 4.1 and 4.2.

The Table below shows the POL results.

PSHA	Soil Strength Factor	Geologic Formation	Magnitude Scaling Factor	POL LIQHAZ		
				P[L] Model Silty Sand	P[L] Model Undifferentiated	P[L] Model Clean Sand
EPRI	1.9	Tobacco Rd.	Arango	6.63e-6	4.36e-6	3.59e-6
LLNL	1.9	Tobacco Rd.	Arango	4.72e-5	3.50e-5	2.97e-5
USGS	1.9	Tobacco Rd.	Arango	1.07e-4	8.91e-5	7.81e-5

POL is computed using each of three Liao et al. (1988) probability models: silty sand, clean sand and undifferentiated. From the Table above we note that the computed probability of liquefaction increases going from clean to silty sands and is contrary to engineering experience: increased fines content generally decreases the probability of liquefaction. However, according to the Liao et al. (1988) contours of equal probability of liquefaction, lower CSRs (< 0.1) are associated with higher POL for silty sands as compared to clean sands (see Figures 1a and 1b). Because a majority of the POL contributions in LIQHAZ come from relatively low induced CSRs, the total POL computed for silty sands is less than that computed for clean sands. This result decreases our confidence in the partitioning of silty and clean sand. Consequently, the Liao et al. undifferentiated probability model is preferred. However, the results for each of the three POL assessments, (EPRI, LLNL and USGS) for any of the three Liao et al. models suggest that the PC-3 performance goal of 1e-4 is met for H-Area.

The H-Area POL disaggregation by earthquake magnitude is given in the Table below. The POL by magnitude (Mw) is given as a percentage of the total. The indicated magnitude is the centroid of the magnitude bin.

EPRI		**LLNL**		**USGS**	
Mw	POL %	Mw	POL %	Mw	POL %
4.75	0.08	5.25	1.27	4.75	0.01
5.25	1.11	5.75	5.07	5.25	0.08
5.9	15.3	6.25	15.1	5.75	0.49
6.7	51.8	6.75	42.5	6.25	2.21
7.8	31.8	7.5	36.1	6.75	2.18
				7.5	95.0

Note: magnitude disaggregation is for "undifferentiated" Liao et al. (1988) model. The percentages do not add to 100% because of round-off.

Note the substantial difference in the USGS magnitude composition as compared to EPRI and LLNL. The large contribution to the USGS Mw 7.5 magnitude bin is the Charleston characteristic earthquake source (Mw 7.3). The EPRI and LLNL PSHAs used a distribution of earthquake magnitudes to describe the Charleston seismic source. We believe that a preferred hazard model would contain a weighted combination of magnitude distributions.

The contribution to the POL by various terms in Equation 1 is illustrated in Figures 14a-d for the EPRI PSHA. The cumulative POL should have small contributions at low control motion because although the probability of occurrence of motion is high, the liquefaction potential is very low. The cumulative POL should have small contributions at high control motions because although the liquefaction potential may be relatively high, the probability of ground motion occurrence is very low. Thus, the contributions to the POL should be small at the high and low ends of control motion used in the analysis, otherwise, the POL could be significantly underestimated. Figure 14a shows the probability of occurrence (POO) by loop index number (term (2) of Equation 1). The sum index runs from 1 to 31 for increasing levels of bedrock motion, 1 to 5 for increasing magnitude bins, and 1 to 6 for increasing distance bins. Thus the total number of POL bins are 31 x 5 x 6 = 930 (Note that the summations on CSR and $(N_1)_{60}$ are not expressed in these figures). Figure 14a illustrates that the POO decreases as a function of increasing bedrock motion and that there is a strong dependence on the magnitude/distance disaggregation (which is why the bin contributions are not smoothly decreasing). Figure 14b illustrates the POL given the CSRN and soil capacity by loop index (term (1) of Equation 1). The increasing POL for increasing bedrock motion and magnitude are clearly illustrated. The contribution to the POL by loop index number (product of terms (1), (2), (3), and (4) of Equation 1) is illustrated in Figure 14c. This figure shows that a proper range in bedrock motions were considered for the problem as the distribution is complete in its symmetry. The cumulative POL is illustrated in Figure 14d. Similarly, Figure sets 15 and 16 illustrate the POL and cumulative POL for the LLNL and USGS PSHAs. The LLNL and USGS cumulative POL plots also suggest that a complete range of bedrock motions were considered for the problem.

5.0 CONCLUSIONS

Program LIQHAZ was developed to evaluate POL and to make an independent evaluation for comparison to an earlier ITP POL evaluation (WSRC, 1995). The LIQHAZ POL evaluations used input data similar to that used for the 1995 evaluation. The LIQHAZ-ITP results were somewhat conservative suggesting that although there was general overall agreement with the 1995 ITP POL evaluation, the full hazard disaggregation should always be used for computation of the POL.

Computations of annual POL for H-Area were also completed using existing cone penetration test soundings. The H-Area POL assessments were made using seismic demand consistent with the recent site response evaluation (WSRC, 1997) and three hard-rock PSHAs: EPRI, LLNL and USGS. The three POL evaluations indicate the PC-3 performance goals are met. Since the subsurface conditions in H-Area are generally less favorable than F-Area (in terms of depth to

the water table and shear wave velocity), the results from H-Area would be a bounding (lower bound or highest probability) case.

From these results, we conclude:

1. The PC-3 performance goal of 10^{-4} is met with respect to liquefaction potential in H-Area.
2. The independent liquefaction evaluation for the ITP using the original soil capacity and seismic demand (WSRC, 1995) results in approximately factor of two increase in the POL. This result provides a level of confidence in the implementation of the liquefaction methodology and an indication that the full hazard dissaggregation should always be used to avoid underestimating the POL.
3. A new POL assessment for the ITP using seismic demand consistent with the SRS site-wide spectra (WSRC, 1997) is consistent with the 1995 estimate of POL using the same EPRI PSHA (WSRC, 1995).
4. Future facility-specific POL evaluations should include an assessment of the applicability of the seismic demand and soil capacity. These soil properties include those used to calculate CSR: shear wave velocities, geologic layering, dynamic properties, and those used to determine soil capacity.

Results are documented in calculation K-CLC-H-00156 (WSRC, 2000d), as required by the WSRC E7 Conduct of Engineering and Technical Support Manual. The study was not performed for any particular project and the results should not be used in any facility-specific analysis. However, if a facility requires the annual liquefaction hazard to be determined, this study demonstrates the methodology for determining POL.

6.0 FUTURE CONSIDERATIONS

1. Because some proposed SRS facilities are to meet Nuclear Regulatory Commission (NRC) design criteria, it would be prudent to re-evaluate the POL for H-Area using NRC seismic criteria. This evaluation would incorporate the median rather than the mean PSHA. Both the EPRI and LLNL median PSHAs are available and could be incorporated in the analysis.
2. An alternative to the magnitude-scaling factor should be explored. The hazard disaggregation is by magnitude and distance bins and as such, ground motion duration and number of cycles of motion may be used directly.
3. Probabilistic models utilizing CPTU data directly, as opposed to converting CPTU data to $(N_1)_{60}$, should be developed.
4. Other methodologies that evaluate probability of liquefaction based on accepted criteria (e.g., shear wave velocity or energy-based methods) should be compared to the Liao et al. models used herein.
5. Important assumptions were made in the computation of liquefaction. The available database of site-specific CSR distributions was derived using a limited range of control motions. The control motion range is exceeded in the PSHAs used in this analysis. For the H-Area computations, extrapolations were made of the CSR distributions, however, an estimated 10% of the POL contributions are from extrapolated ranges of the CSRs. For future site-

specific work, we recommend that the site-specific CSR distributions be complemented with higher ranges of bedrock control motions to avoid extrapolation.

6. POL maps could be generated that can assist mitigation efforts by providing a greater understanding of an earthquake's impact on emergency services and lifelines in and around the SRS.

7.0 REFERENCES

Arango, I., 1994. *Methodology for Liquefaction Potential Evaluation of Sites East of the Rockies*, Bechtel Corporation, Technical Grant, June 1994.

Arango, I., 1996. *Magnitude Scaling Factors for Soil Liquefaction Evaluations*, Journal of Geotechnical Engineering, ASCE, Vol. 122, No. 11, pp. 929-936, November 1996.

Bernreuter, Don L., 1997. Letter from Don Bernreuter of Lawrence Livermore National Laboratory to Jeff Kimball of U. S. Dept. of Energy, Re: transmittal of rock hazard results for Savannah River Site, May 15, 1997.

Frankel, A., 1999. Letter from A. Frankel of USGS to R. C. Lee, Re: Results of USGS calculation of SRS PSHA, March 1, 1999.

Liao, Samson S. C., and Robert V. Whitman, 1986. *Overburden Correction Factors for SPT in Sand*, Journal of Geotechnical Engineering, ASCE, Vol. 112, No. 3, pp. 373-377.

Liao, Samson S. C., Veneziano, D., and Robert V. Whitman, 1988. *Regression Models for Evaluating Liquefaction Probability*, Journal of Geotechnical Engineering, ASCE, Vol. 114, No. 4, pp. 389-411.

NCEER, 1997. *Proceedings of the NCEER Workshop on Evaluation of Liquefaction Resistance of Soils*, National Center for Earthquake Engineering Research, Technical Report No. NCEER-97-0022, State University of New York at Buffalo, New York, December 31, 1997.

NEI, 1994. *Seismic Siting Decision Process*, Nuclear Energy Institute, Washington, D. C., May 24, 1994.

Savy, J. B., 1996. Letter from J. B. Savy, Deputy Associate Program Leader Natural Phenomena Hazards, to Jeff Kimball, U. S. Department of Energy, Re: *Fission Energy and Systems Safety Program*, Correspondence No. SANT96-147JBS, April 24, 1996.

Seed, H. B., Tokimatsu, K., and L. F. Harder Jr., 1984. *The Influence of SPT Procedures in Evaluating Soil Liquefaction Resistance*, Report No. UCB/EERC-84-15, University of California at Berkeley, Berkeley, California.

Singh, S., Seed, H. B., and C. K. Chan, 1979. *Undisturbed Sampling and Cyclic Load Testing of Sands*, Report No. UCB/EERC-79/33, University of California at Berkeley, Berkeley, California.

WSRC, 1993. *Savannah River Site Replacement Tritium Facility (233H), Geotechnical Investigation*, WSRC-RP-93-606, April 1993.

WSRC, 1995. *In Tank Precipitation Facility (ITP) and H-Tank Farm (HTF) Geotechnical Report*, WSRC-TR-95-0057, Rev. 0, September 1995.

WSRC, 1996. *Investigations of Nonlinear Dynamic Soil Properties at the Savannah River Site*, WSRC-TR-96-0062, Rev. 0, March 1996.

WSRC, 1997. *SRS Seismic Response Analysis and Design Basis Guidelines*, WSRC-TR-97-0085, Rev. 0, March 31, 1997.

WSRC, 1998. *Soil Surface Seismic Hazard and Design Basis Guidelines for Performance Category 1 & 2 SRS Facilities*, WSRC-TR-98-00263, Rev. 0, September 30, 1998.

WSRC, 1999. *Computation of USGS Soil UHS and Comparison to NEHRP and PC1 Seismic Response Spectra for the SRS*, WSRC-TR-99-0271, Rev. 0, September 1999.

WSRC, 2000a. *Determination of Stratagraphic Tops for F and H Area Tobacco Road, Dry Branch and Santee Formations*, K-CLC-G-00069, Rev. 0, May 2, 2000.

WSRC, 2000b. *CPTU $(N1)_{60}$ Determination*, K-CLC-G-00067, Rev. 0, August 2000.

WSRC, 2000c. *Estimation of $(N1)_{60}$ Statistics for H-Area Tobacco Road Formation Using Piezocone Penetration Test Data*, K-CLC-H-00157, Rev. 0, August 2000.

WSRC, 2000d. *Probability of Liquefaction Calculated Using Computer Program LIQHAZ*, K-CLC-H-00156, Rev. 0, August 2000.

Table 1. Magnitude Scaling Factors

Earthquake Magnitude	Magnitude Scaling Factor
8.25	0.63
8	0.75
7.5	1.00
7	1.25
6	2.00
5.5	3.00

(Arango, 1994; 1996)

Table 2. Input Matrix for Various POL Computations

Computer Program/Code	Case	Seismic Demand CSR	Soil Capacity $(N_1)_{60}$	Soil Strength Factor	MSF	PSHA	Geologic Formation	Water Table	P[L] Model	POL
ASHLE ITP (see Section 4.1)	1	ITP original	ITP original	1.9	Arango	EPRI	Tobacco Rd.	ITP Original	Silty Sand	2.25e-6
LIQHAZ ITP (see Section 4.1)	1	ITP original	ITP original	1.9	Arango	EPRI	Tobacco Rd.	ITP Original	Silty Sand	4.90e-6
LIQHAZ ITP (see Section 4.1)	2	ITP original	ITP original	1.9	Arango	LLNL	Tobacco Rd.	ITP Original	Silty Sand	3.57e-5
LIQHAZ ITP (see Section 4.2)	3	SRS 1997	ITP CPTU	1.9	Arango	EPRI	Tobacco Rd.	25 ft	Silty Sand	4.98e-6
LIQHAZ H-Area (see Section 4.3)	4	SRS 1997	H-Area CPTU	1.9	Arango	EPRI	Tobacco Rd.	25 ft	Silty Sand	6.63e-6
LIQHAZ H-Area (see Section 4.3)	4	SRS 1997	H-Area CPTU	1.9	Arango	LLNL	Tobacco Rd.	25 ft	Silty Sand	4.72e-5
LIQHAZ H-Area (see Section 4.3)	4	SRS 1997	H-Area CPTU	1.9	Arango	USGS	Tobacco Rd.	25 ft	Silty Sand	1.07e-4
LIQHAZ H-Area (see Section 4.3)	5	SRS 1997	H-Area CPTU	1.9	Arango	EPRI	Tobacco Rd.	25 ft	Undiff.	4.36e-6
LIQHAZ H-Area (see Section 4.3)	5	SRS 1997	H-Area CPTU	1.9	Arango	LLNL	Tobacco Rd.	25 ft	Undiff.	3.50e-5
LIQHAZ H-Area (see Section 4.3)	5	SRS 1997	H-Area CPTU	1.9	Arango	USGS	Tobacco Rd.	25 ft	Undiff.	8.91e-5
LIQHAZ H-Area (see Section 4.3)	6	SRS 1997	H-Area CPTU	1.9	Arango	EPRI	Tobacco Rd.	25 ft	Clean Sand	3.59e-6
LIQHAZ H-Area (see Section 4.3)	6	SRS 1997	H-Area CPTU	1.9	Arango	LLNL	Tobacco Rd.	25 ft	Clean Sand	2.97e-5
LIQHAZ H-Area (see Section 4.3)	6	SRS 1997	H-Area CPTU	1.9	Arango	USGS	Tobacco Rd.	25 ft	Clean Sand	7.81e-5

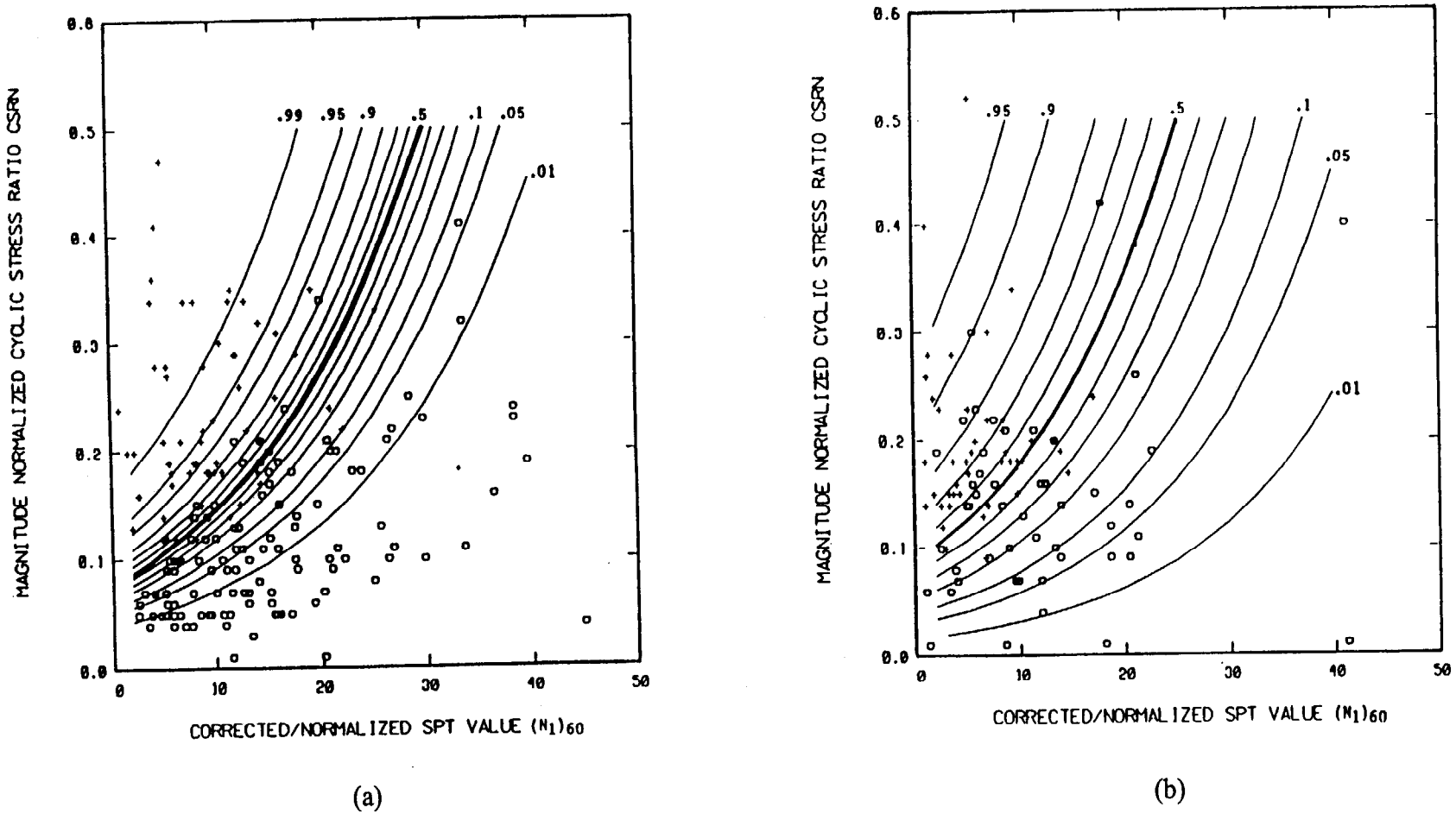

Figure 1. Contours of Equal Probability of Liquefaction for (a) Clean Sand (Fines ≤ 12%) and (b) Silty Sand (Fines >12%)
(Liao et al., 1988)

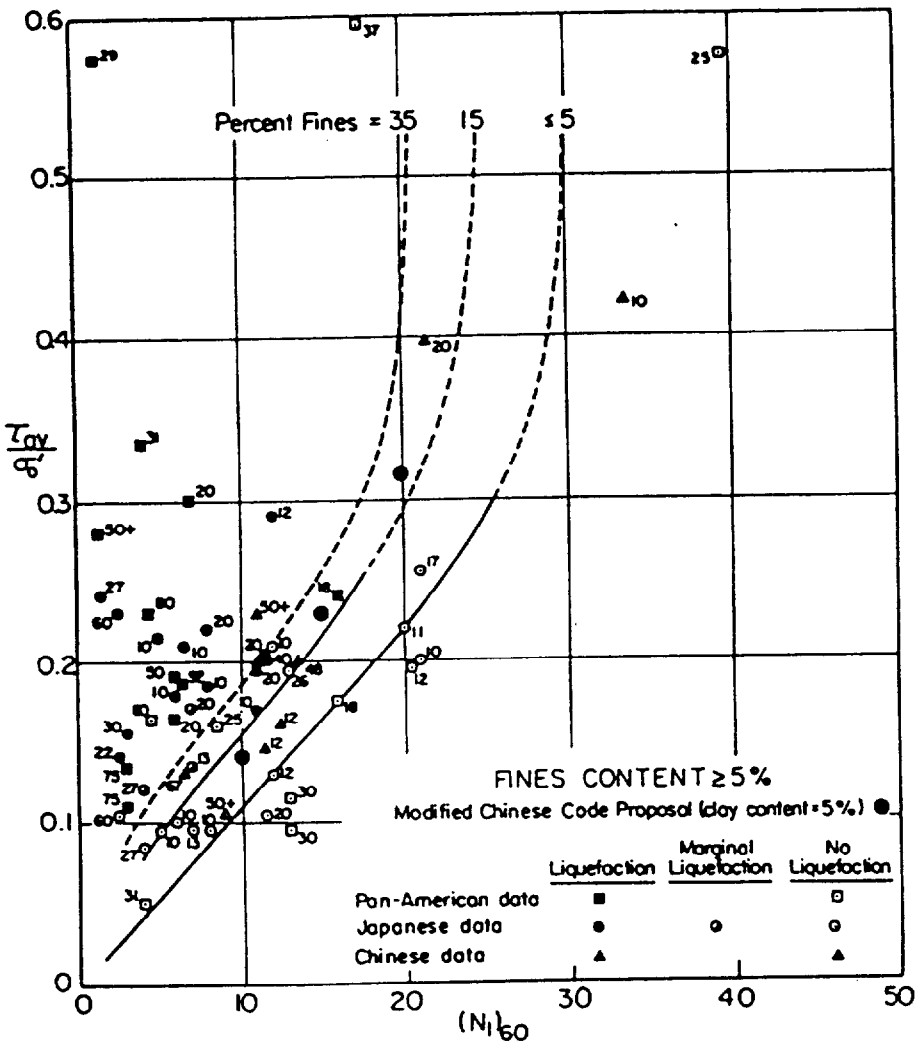

Figure 2. Relationship Between $(N_1)_{60}$, Percent Fines, and CRR (Seed et al., 1984)

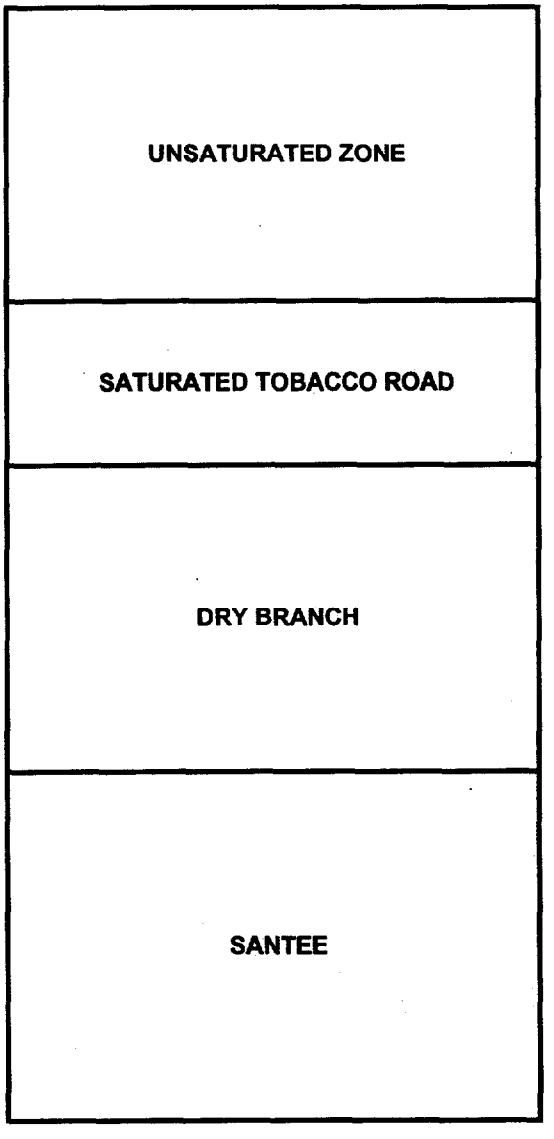

Bottom Elevation (feet MSL)	CPT Calculated $(N_1)_{60}$ (blows per ft)	Tip Stress q_t (tsf)	Cyclic Resistance Ratio CRR
303.7 (±14.9)			
	19.8 (±12.0)	82.2 (±68.7)	0.44 (±0.35)
255.4 (±8.0)			
	13.1 (±5.7)	90.8 (±67.4)	0.22 (±0.17)
228.5 (±8.1)			
	14.5 (±7.2)	140.4 (±96.8)	0.24 (±0.21)
177.7 (±13.9)			
	13.9 (±7.7)	134.4 (±103.9)	0.25 (±0.23)

Numbers shown are average values, numbers in parentheses are standard deviations.

Figure 3. Generalized Cross Section for H-Area

crossect.xls

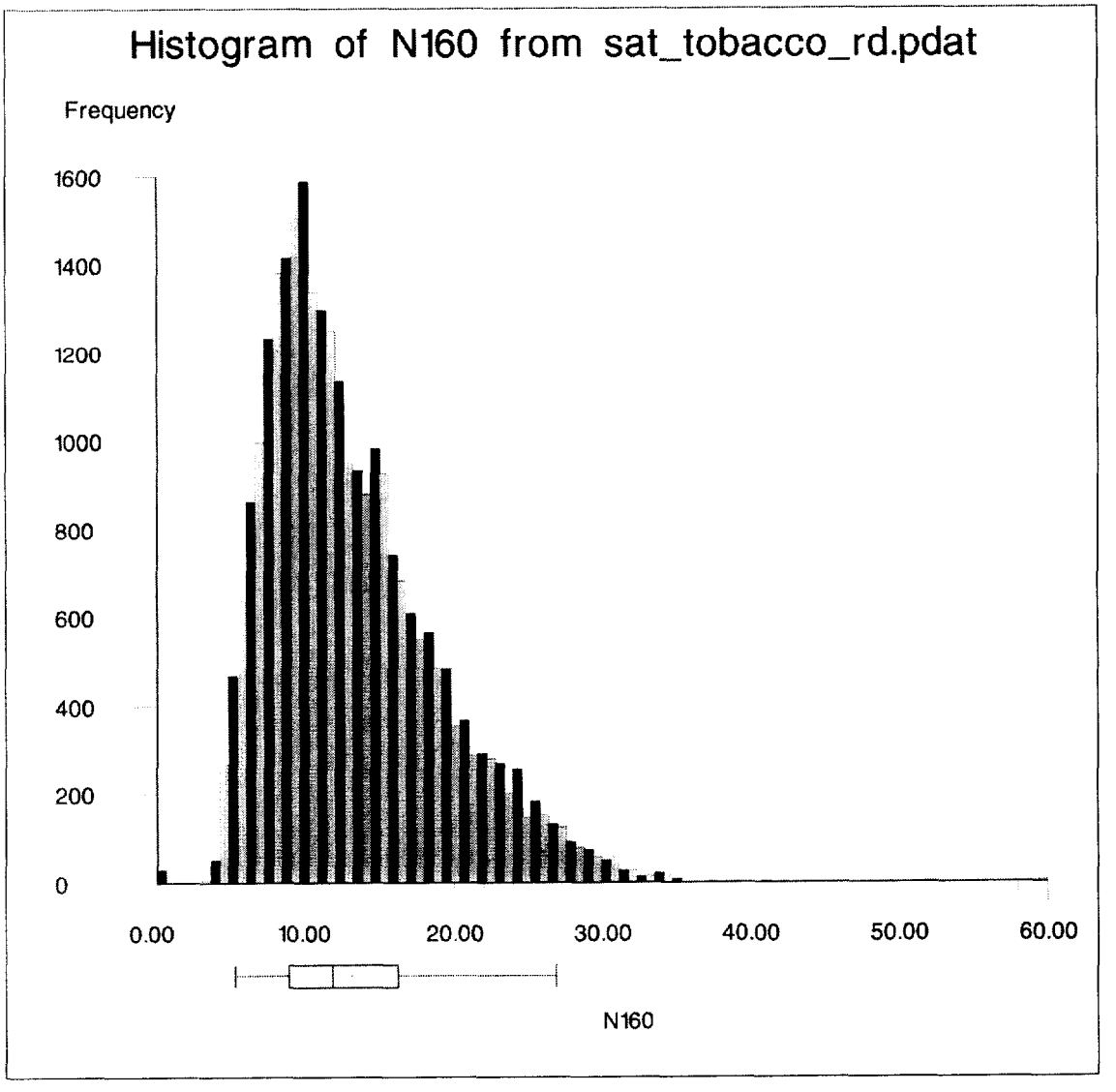

Figure 4. Histogram of CPTU Estimated $(N_1)_{60}$ Values for the H-Area Saturated Tobacco Road Formation
(WSRC, 2000c)

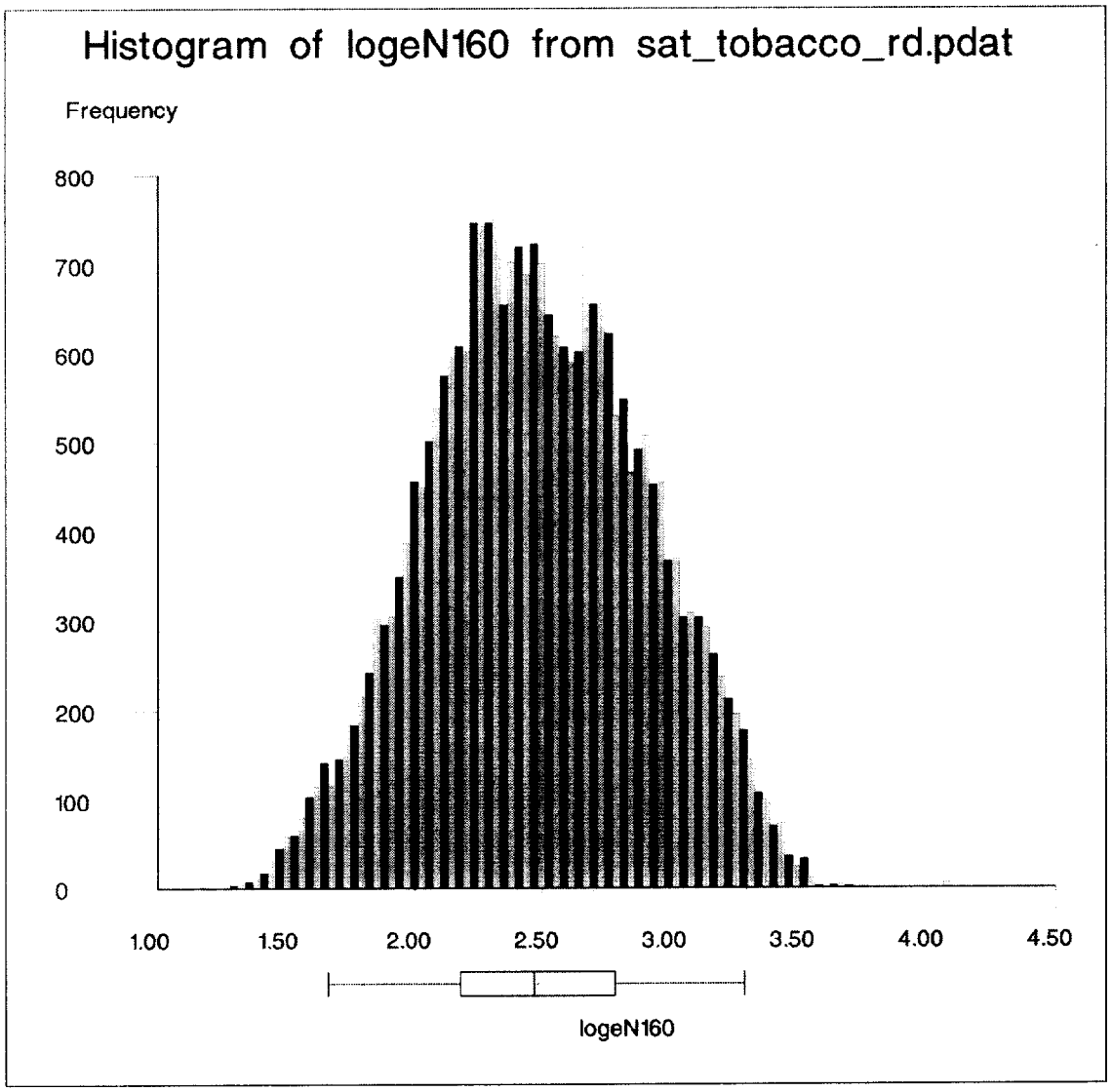

Figure 5. Histogram of CPTU Estimated ln $[(N_1)_{60}]$ Values for the H-Area Saturated Tobacco Road Formation
(WSRC, 2000c)

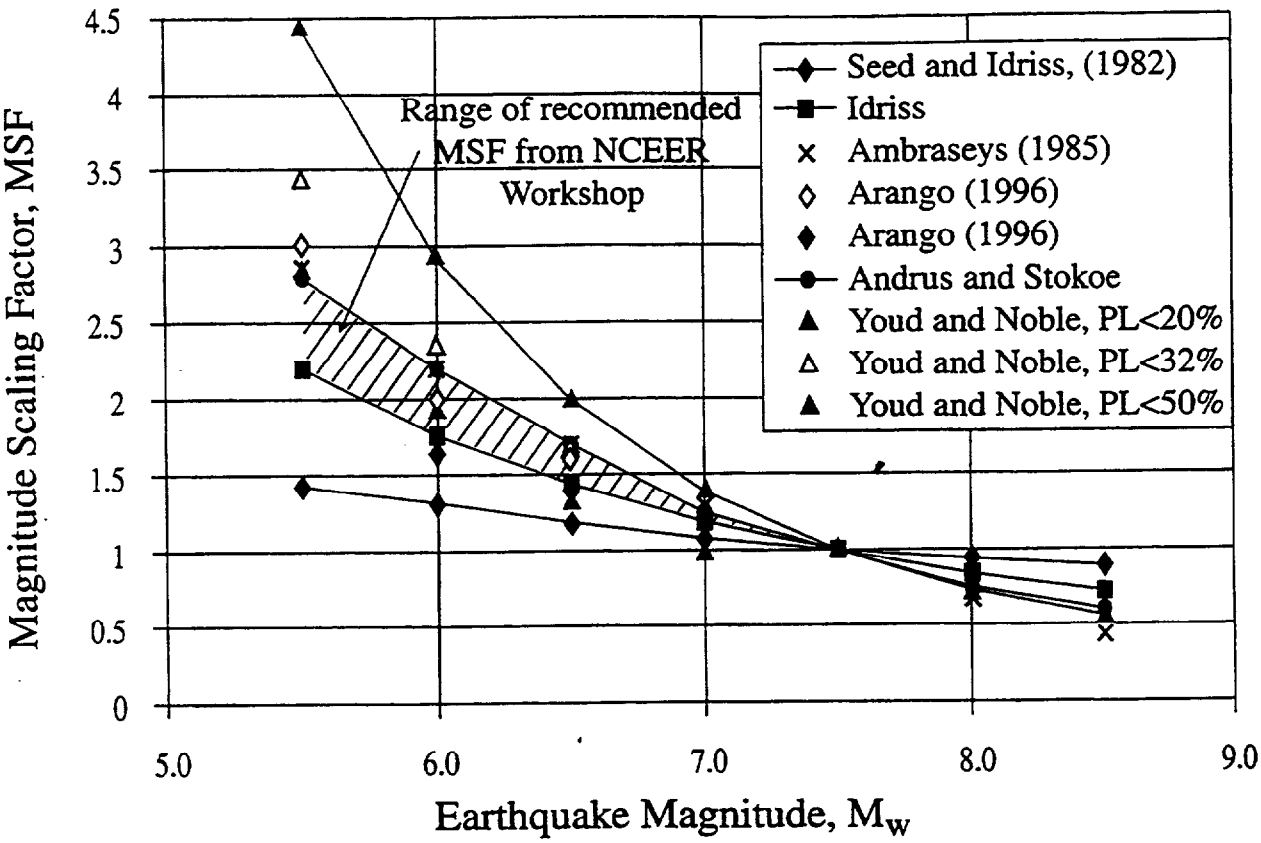

Figure 6. Magnitude Scaling Factors Proposed by Various Investigators (NCEER, 1997)

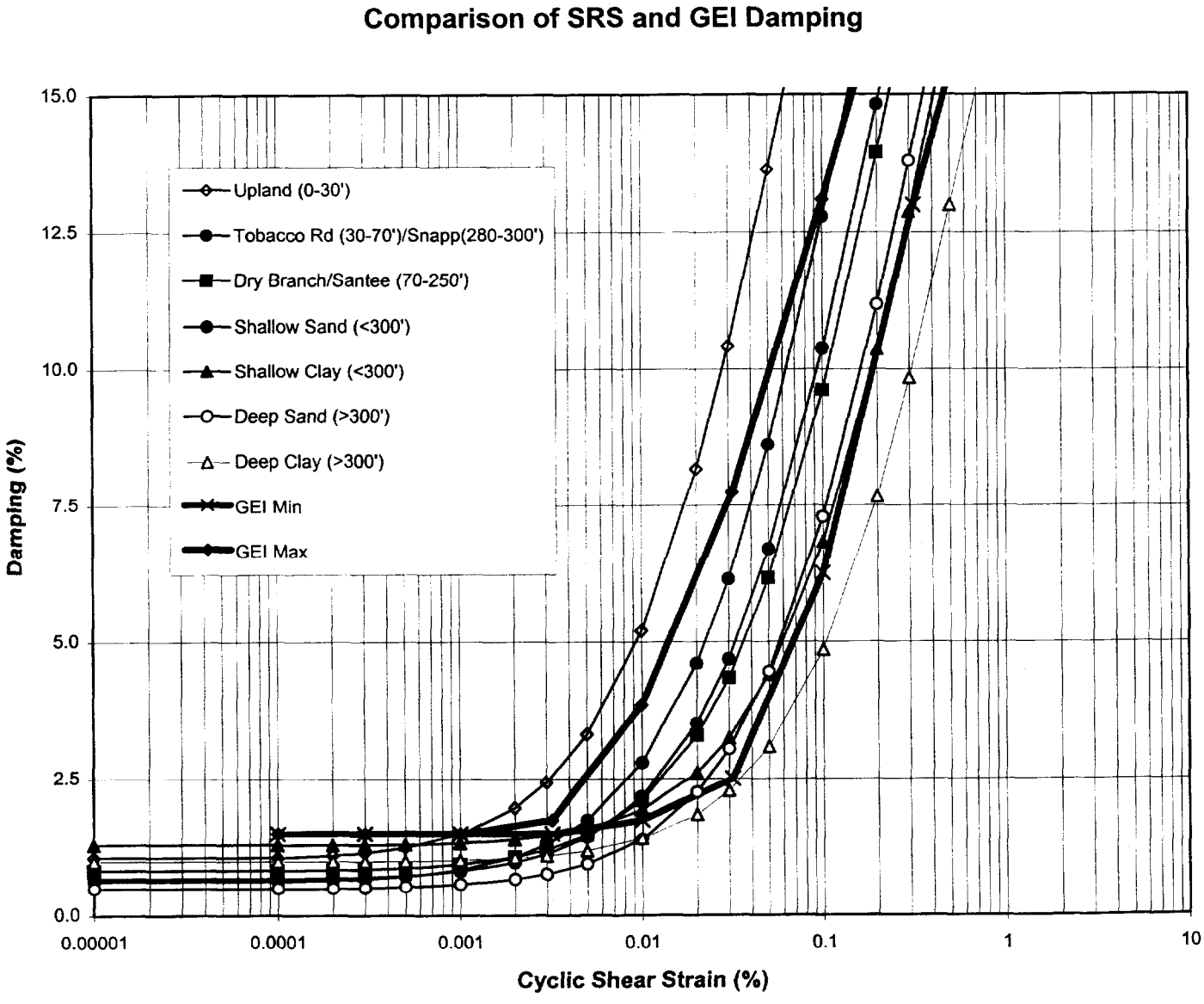

Figure 7. Comparison of SRS "Best Estimate" Damping with GEI Damping (WSRC, 1996)

figure7.XLS

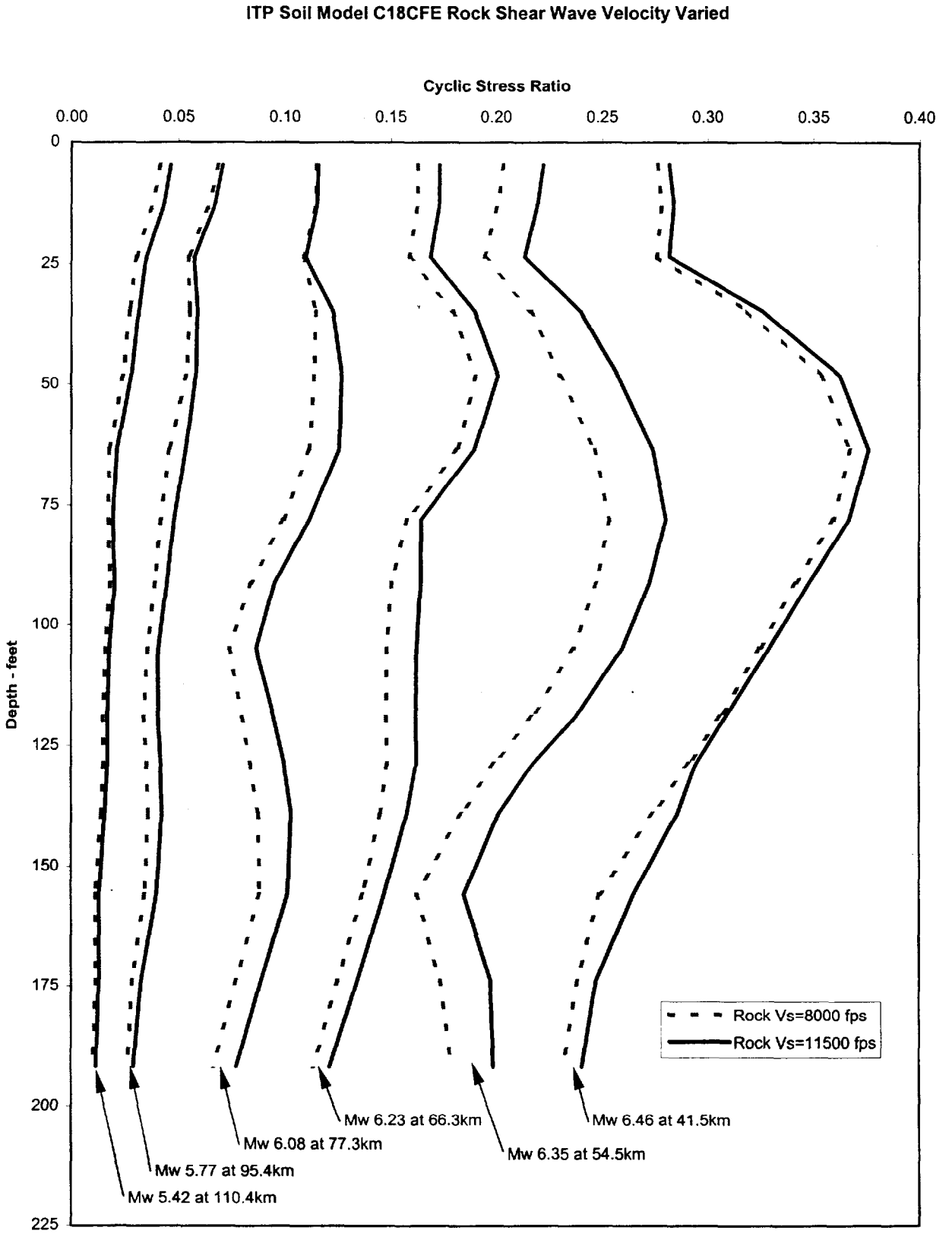

Figure 8. Comparison of ITP Convolution Analyses Using Rock Shear Wave Velocity of 8,000 ft/sec and 11,500 ft/sec

rockvs.xls

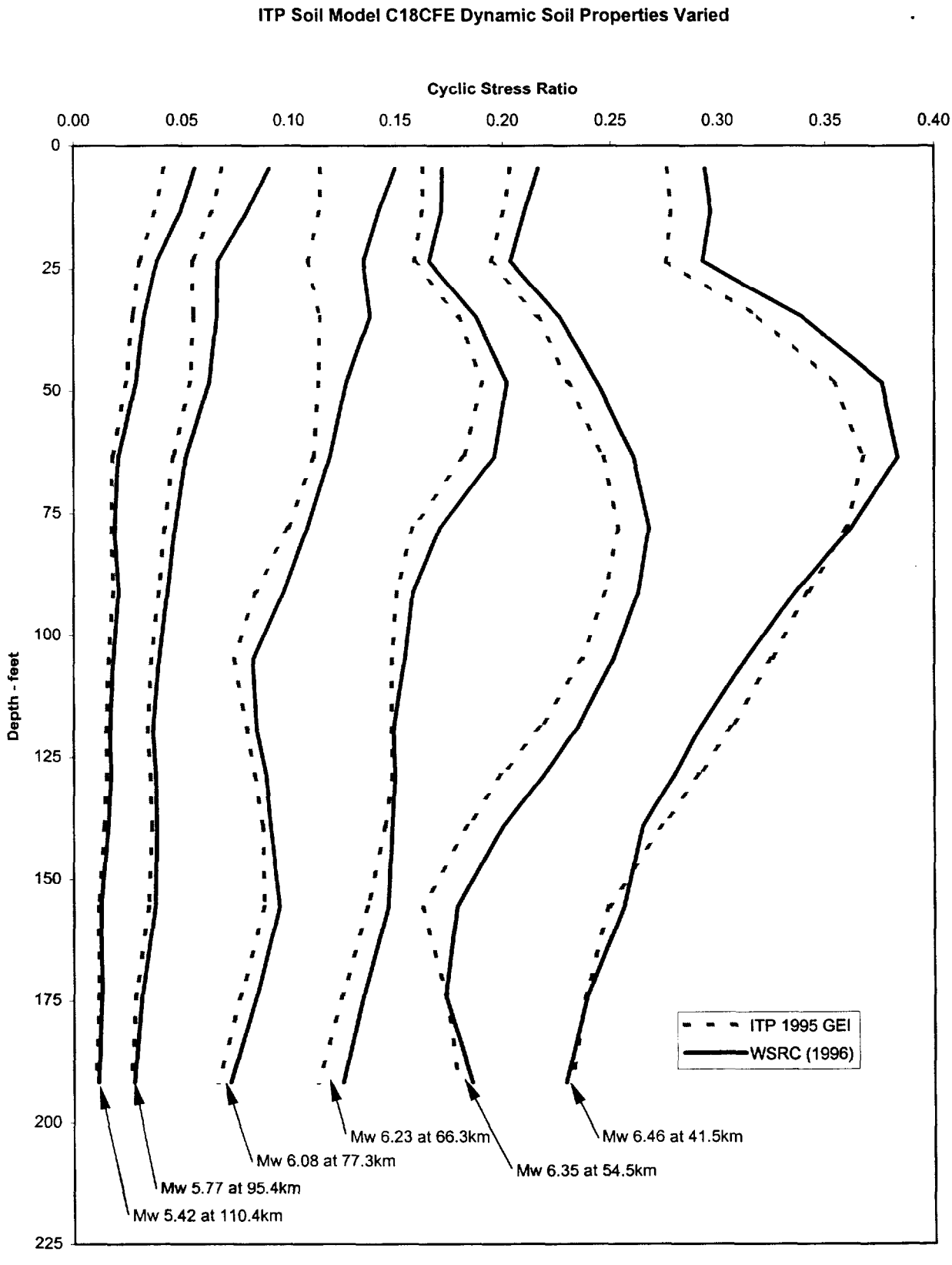

Figure 9. Comparison of ITP Convolution Analyses Using GEI Dynamic Properties and SRS "Best Estimate" Dynamic Properties

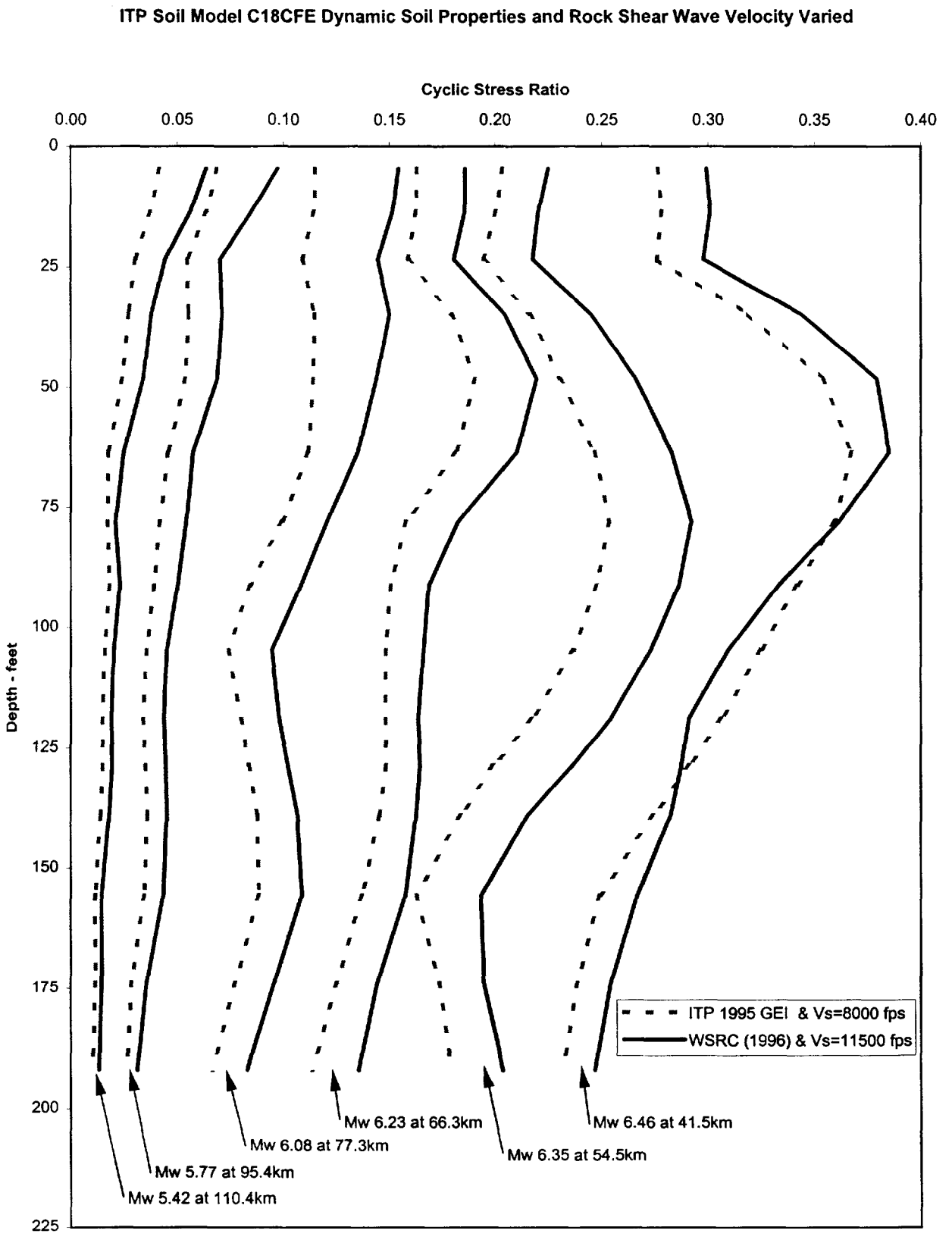

Figure 10. Comparison of Original ITP Convolution Analyses With Revised Analysis Using Shear Wave Velocity of 11,500 ft/sec and SRS "Best Estimate" Dynamic Properties

rk-curve.xls

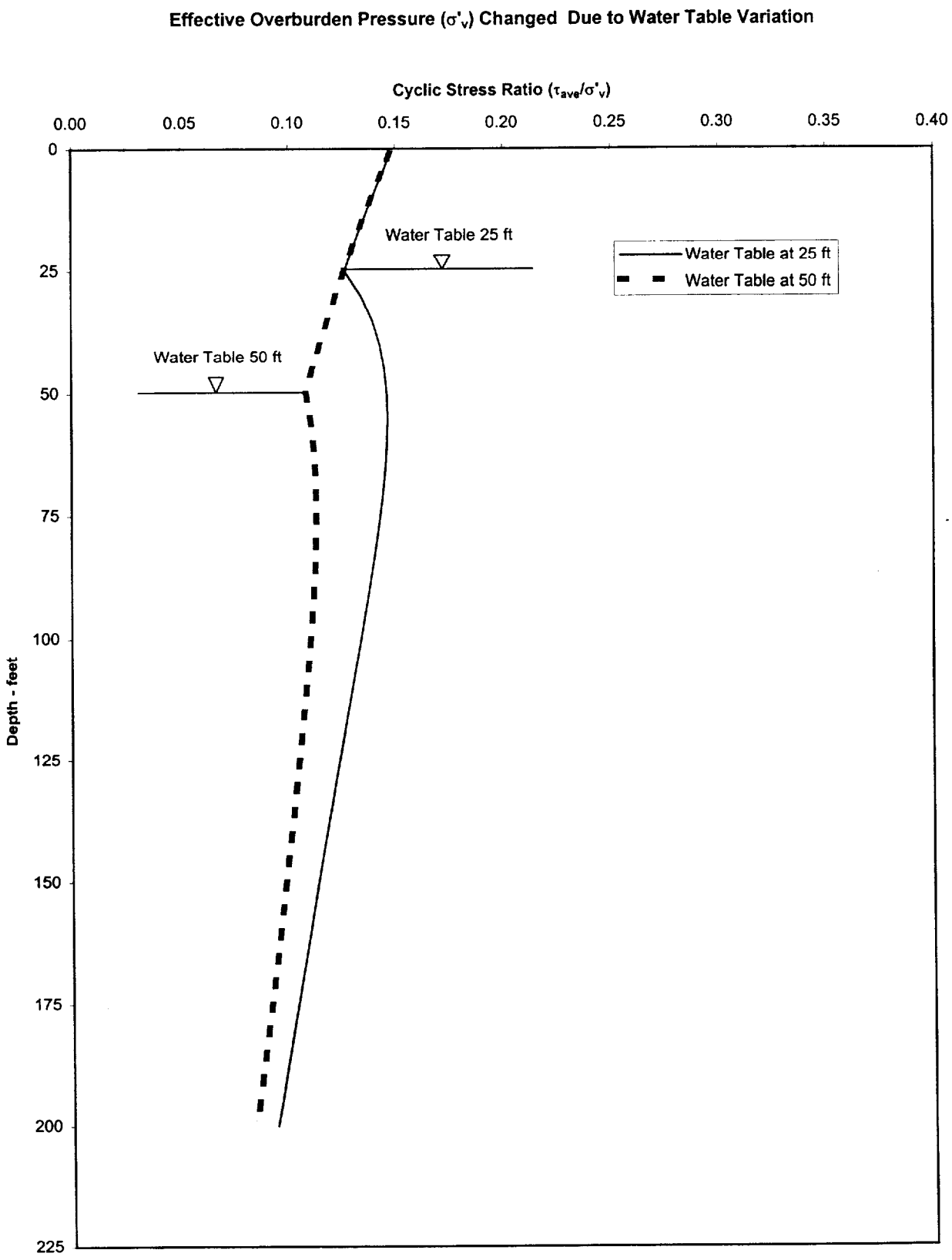

Figure 11. Comparison of Cyclic Stress Ratio for Water Table at 25 and 50 feet

itp7-CSR.xls

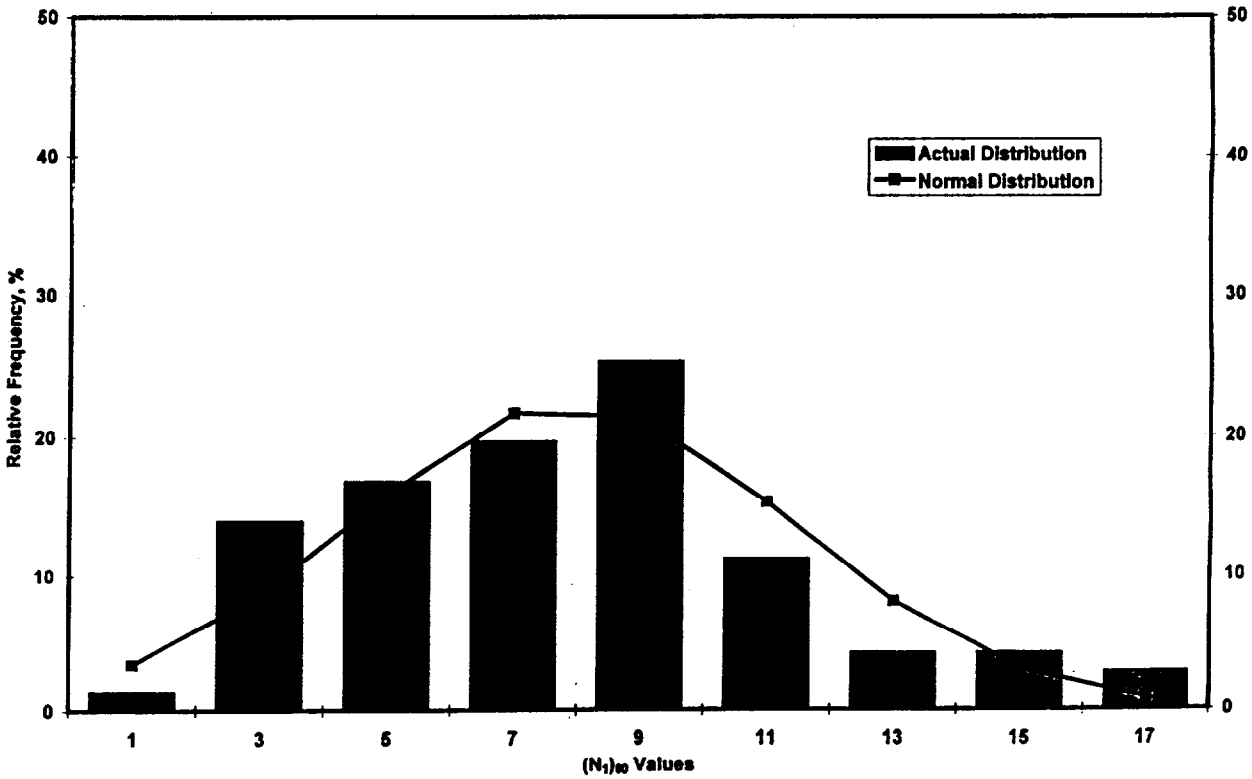

Figure 12. Histogram of ITP $(N_1)_{60}$ values (measured and simulated combined) (WSRC, 1995)

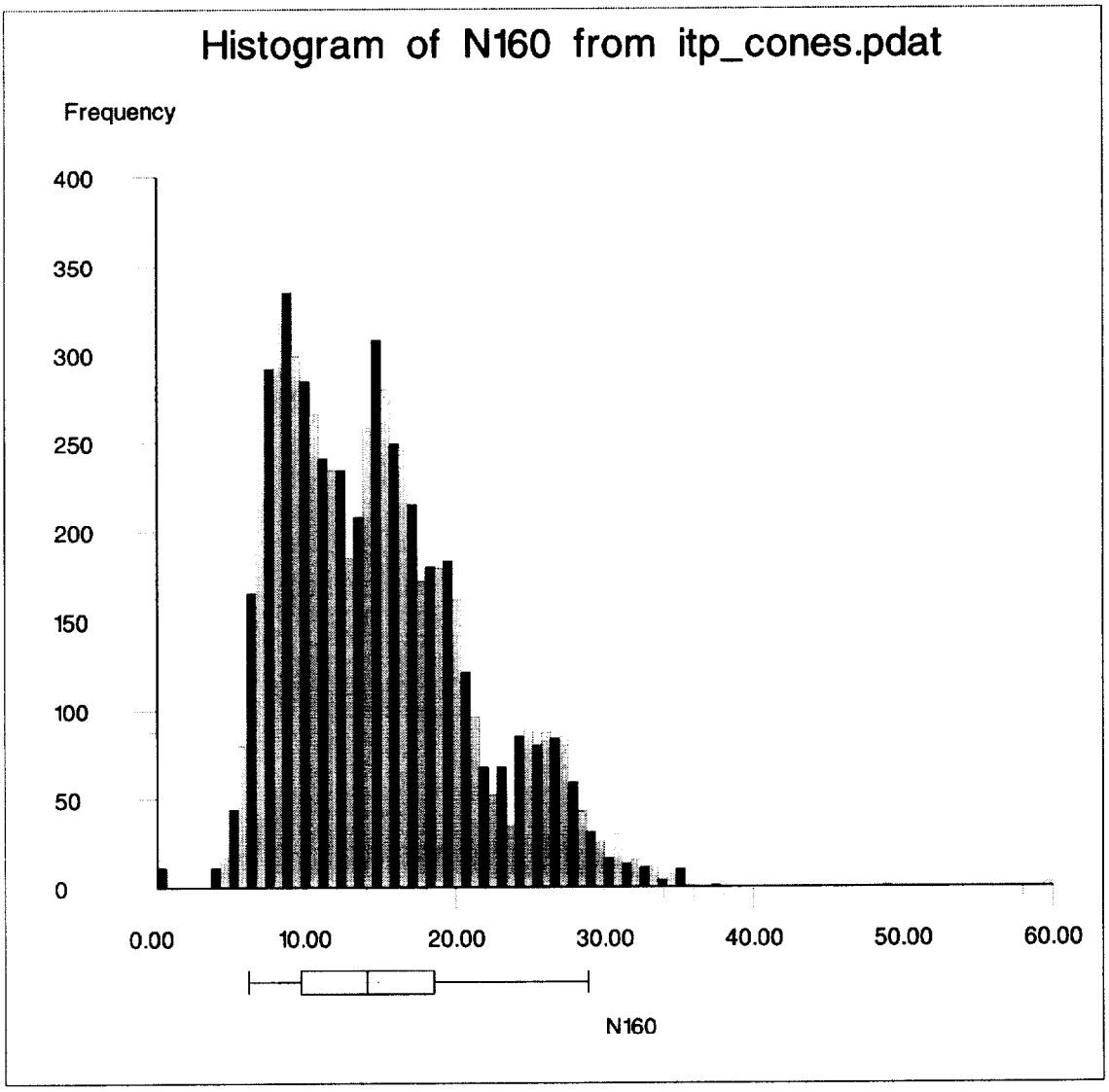

Figure 13. Histogram of $(N_1)_{60}$ Values for Elevations 220 to 250 ft-msl Estimated Using 20 ITP CPTUs and Equations 2 through 4
(WSRC, 2000c)

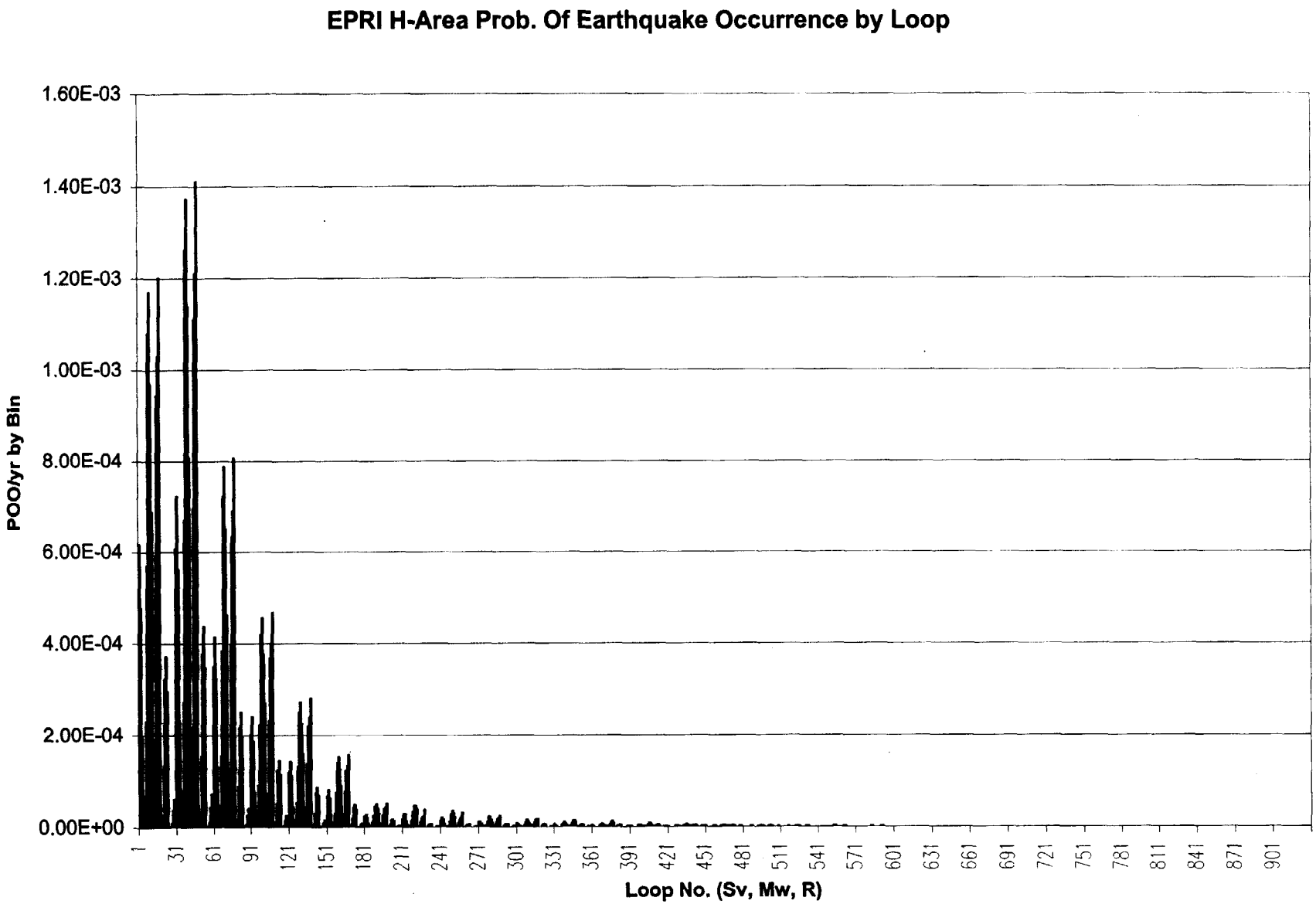

Figure 14a. EPRI H-Area Probability of Earthquake Occurrence by Loop
(see Term 2 Equation 1, page 6)

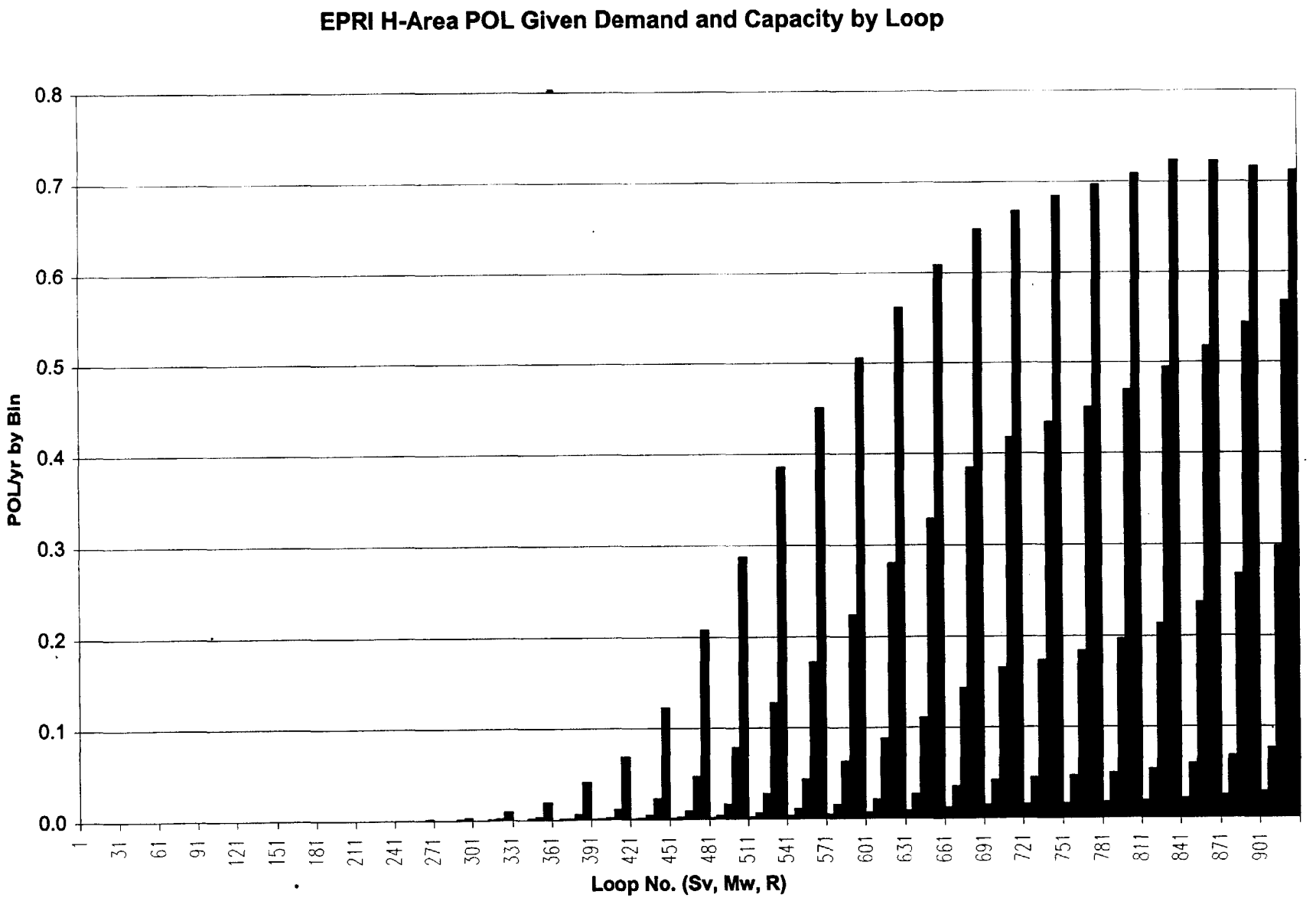

Figure 14b. EPRI H-Area Probability of Liquefaction Given CSRN and $(N_1)_{60}$ by Loop
(see Term 1 Equation 1, page 6)

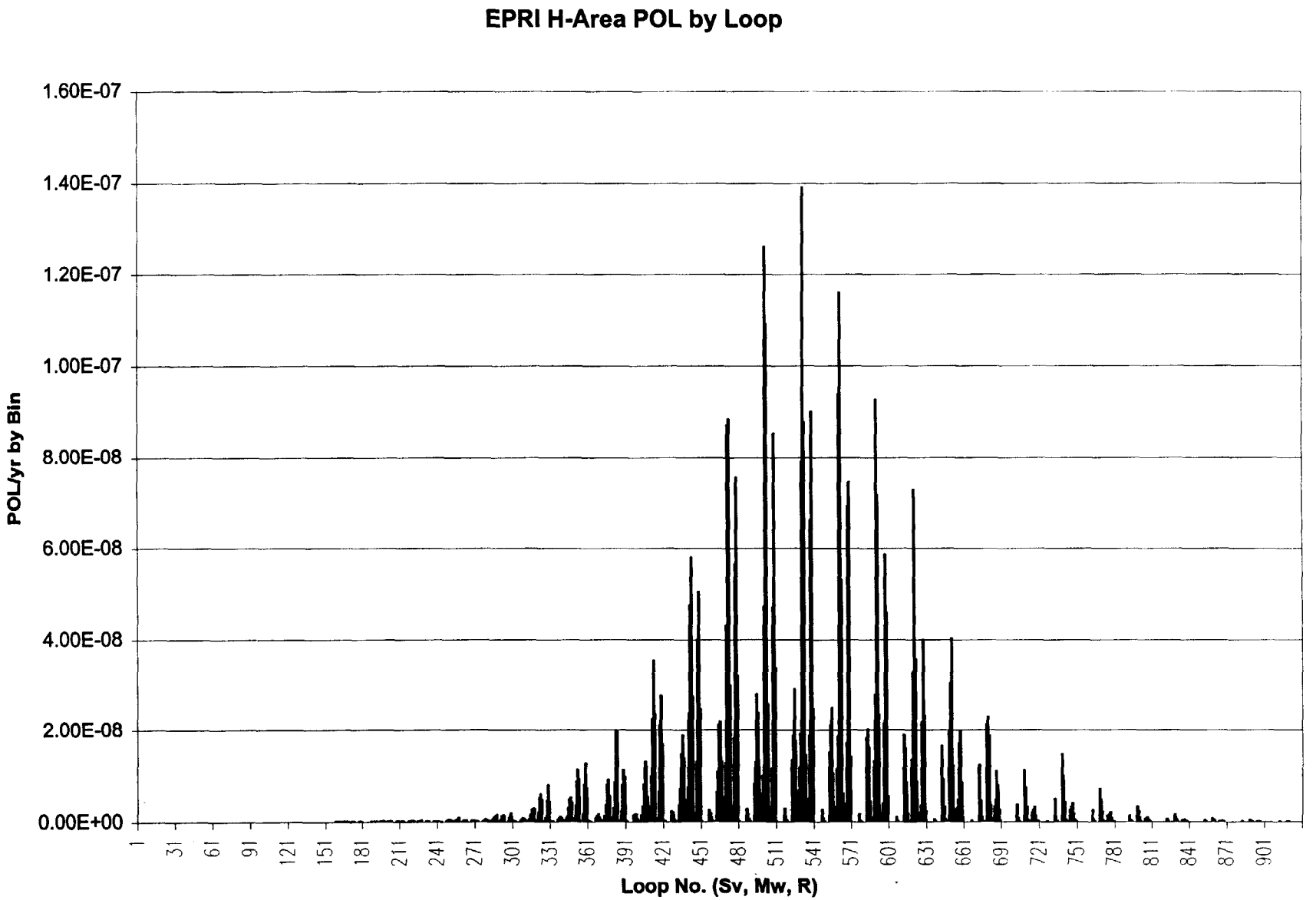

Figure 14c. EPRI H-Area Probability of Liquefaction by Loop
(Product of Terms (1), (2), (3), and (4) Equation 1, see page 6)

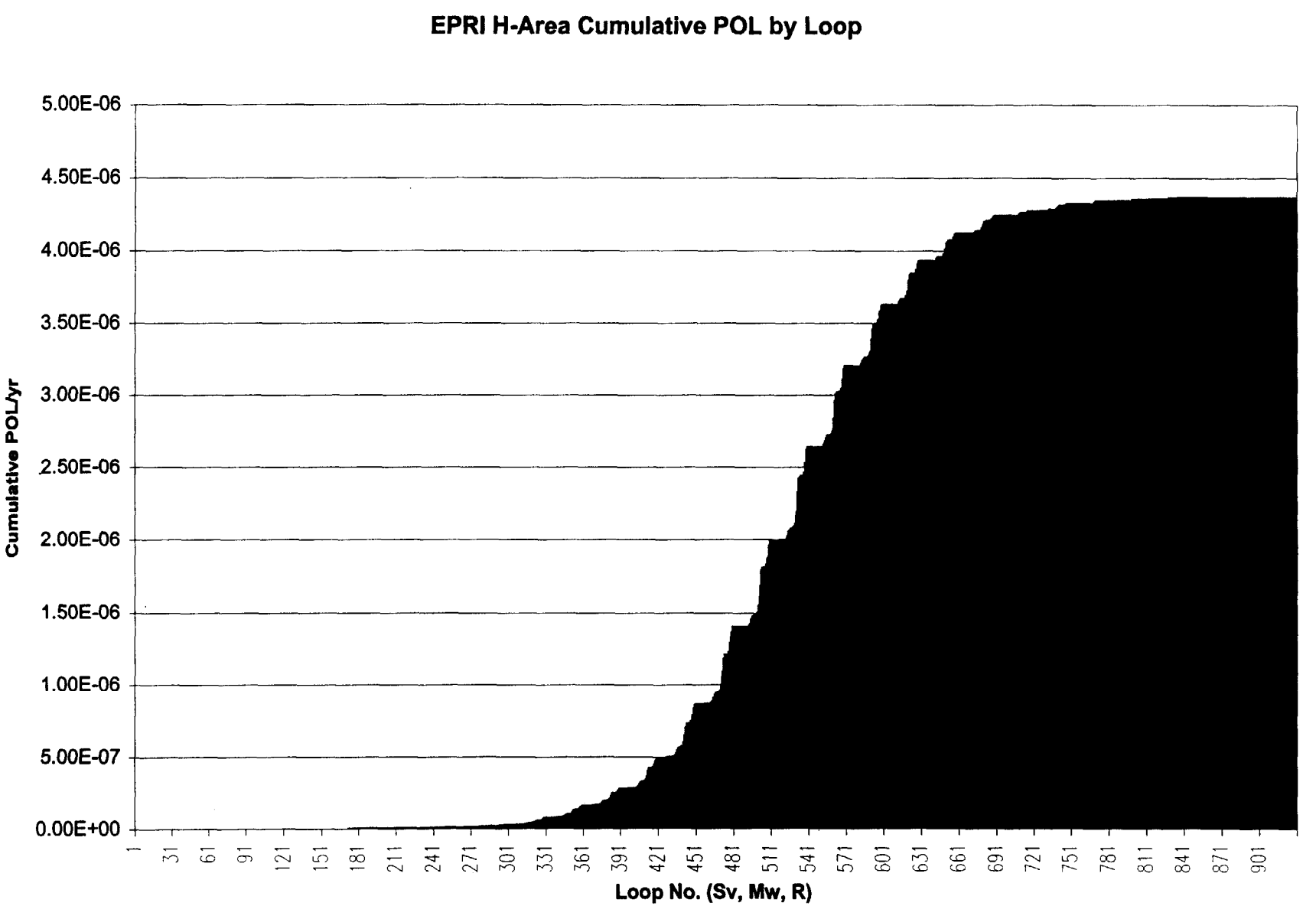

Figure 14d. EPRI H-Area Cumulative Probability of Liquefaction Summed by Loop
(Equation 1, see page 6)

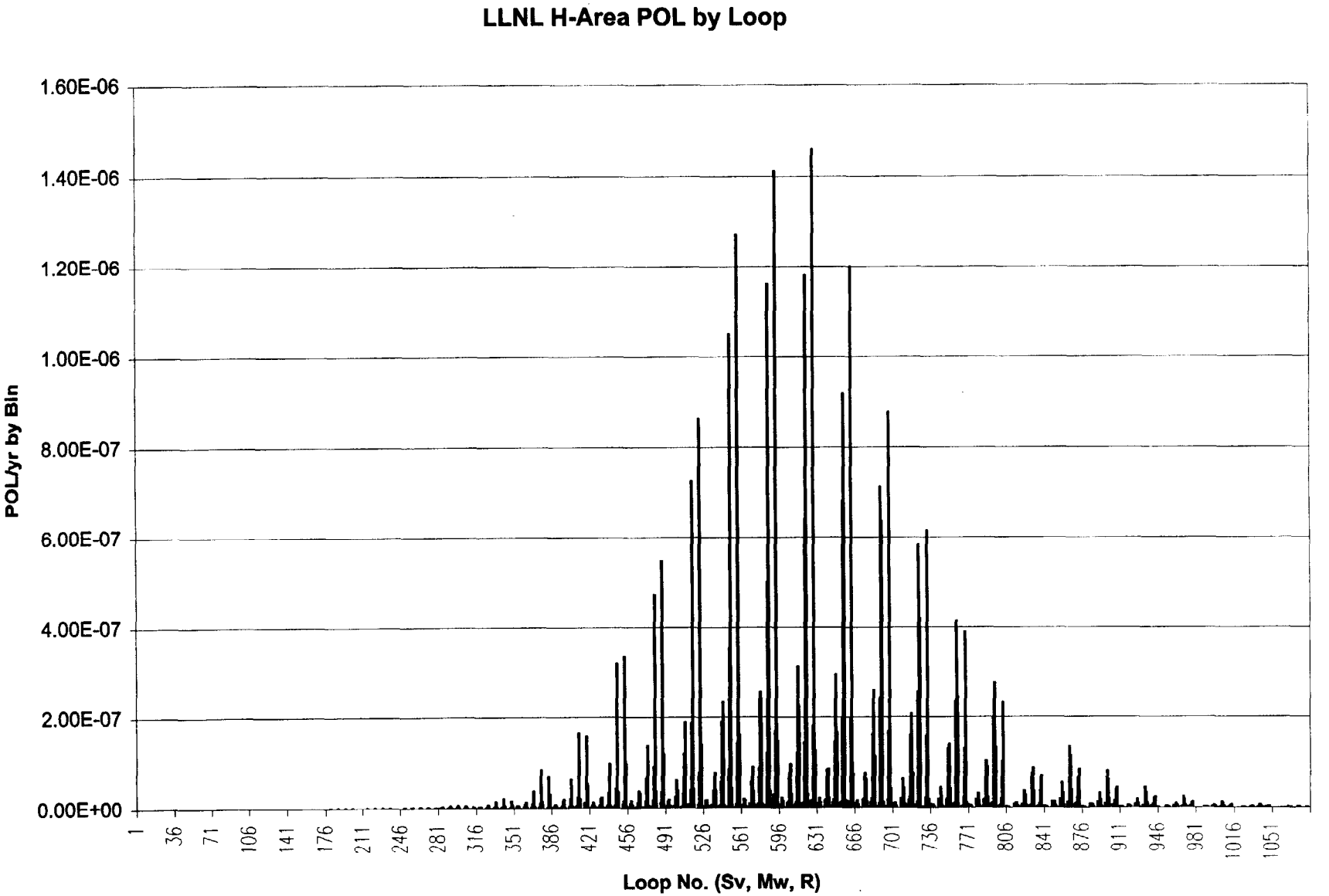

Figure 15a. LLNL H-Area Probability of Liquefaction by Loop
(Product of Terms (1), (2), (3), and (4) Equation 1, see page 6)

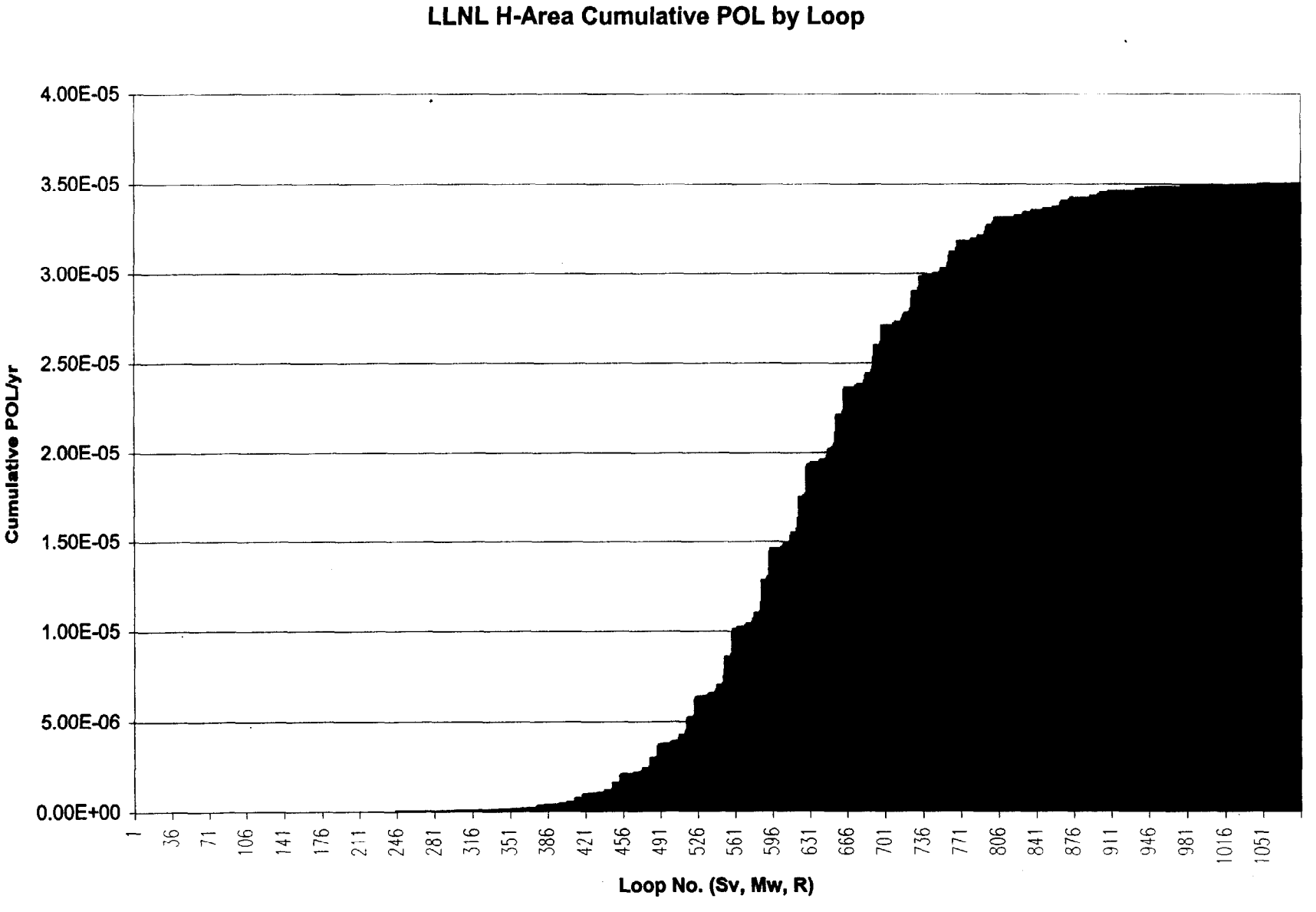

Figure 15b. LLNL H-Area Cumulative Probability of Liquefaction Summed by Loop
(Equation 1, see page 6)

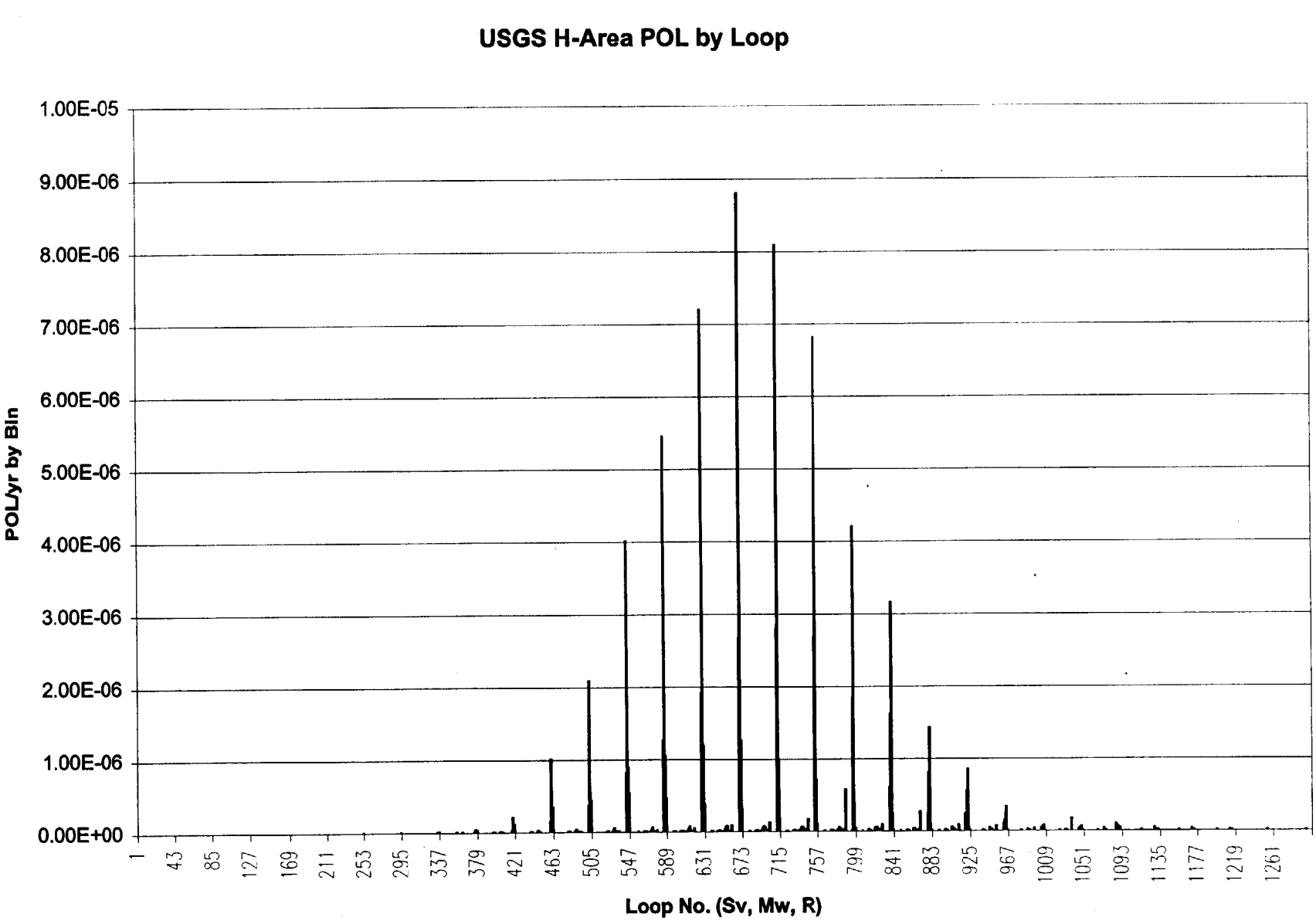

Figure 16a. USGS H-Area Probability of Liquefaction by Loop
(Product of Terms (1), (2), (3), and (4) Equation 1, see page 6)

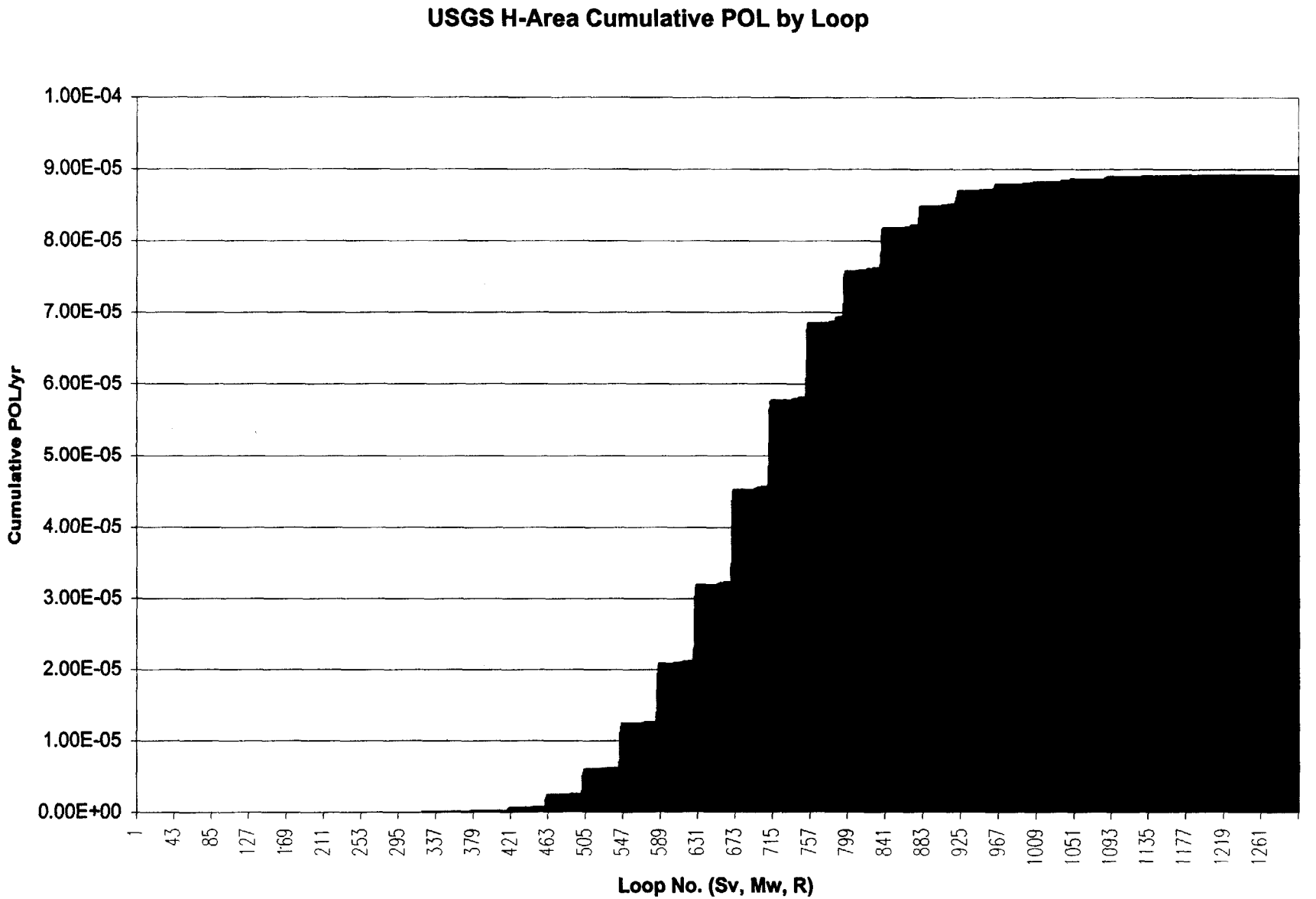

Figure 16b. USGS H-Area Cumulative Probability of Liquefaction Summed by Loop
(Equation 1, see page 6)